

Receptive Field Properties of Neurons in Area V3 of Macaque Monkey Extrastriate Cortex

DANIEL J. FELLEMAN AND DAVID C. VAN ESSEN

*Division of Biology 216-76, California Institute of Technology,
Pasadena, California 91125*

SUMMARY AND CONCLUSIONS

1. Receptive field properties of 147 neurons histologically verified to be located in area V3 were investigated during semichronic recording from paralyzed anesthetized macaque monkeys. Quantitative analyses were made of neuron selectivities for direction, orientation, speed, binocular disparity, and color.

2. The majority of neurons in V3 (76%) were strongly orientation selective; 40% demonstrated strong direction selectivity. Most cells were tuned for stimulus speed and almost half showed optimum responses at $16^{\circ}/\text{s}$. The distribution of optimum speeds ranged primarily from 4 to $32^{\circ}/\text{s}$.

3. Several cells in V3 displayed multi-peaked orientation- and/or direction-tuning curves. These cells had two or more narrowly tuned peaks that were not co-axial. In some ways, they resemble higher-order hypercomplex cells of cat area 19 (40) and may subserve a higher level of form or motion analysis than is seen at antecedent visual areas.

4. Roughly half (45%) of the cells were selective for binocular disparity. Approximately half of these were tuned excitatory in that they showed weak responses when tested through either eye alone, but showed strong binocular facilitation centered on the fixation plane. The other disparity-selective cells were tuned inhibitory or asymmetric in their responses in front and behind the fixation plane.

5. Contrary to previous reports, ~20% of the neurons in V3 were color selective in terms of showing a severalfold greater response to the best monochromatic wavelength compared with the worst. Color-tuning curves of the subset of color selective cells had, on av-

erage, a full bandwidth at half maximum response of 80–100 nm.

6. A comparison of the receptive field properties of neurons in V3 to those in other areas of visual cortex suggests that V3, like MT, is well suited for the analysis of several aspects of stimulus motion. V3 may also be involved in some aspects of form analysis, particularly at low contrast levels. Comparison with area VP, a thin strip of cortex anterior to ventral V2, which was previously considered part of V3, indicates that direction selectivity is much more prevalent in V3 than in VP. Conversely, color-selective cells are the majority in VP but a minority in V3. This suggests that visual information is processed differently in the upper and lower visual fields.

INTRODUCTION

The visual cortex of macaque monkeys comprises many distinct areas that can be recognized on the basis of architecture, topography, connections, and functional properties (76). The laminar patterns of connections among these areas has been used to hypothesize an anatomical hierarchy of visual cortical areas (78). This cortical hierarchy contains many parallel pathways, several of which have been suggested to participate in distinct “functional streams” through visual cortex (75).

This report concerns the receptive field properties of cells in area V3, which is located immediately anterior to V2 in dorsal extrastriate cortex. A physiological study of V3 is of particular interest for several reasons. First, V3 is located at the third level of the visual

cortical hierarchy and thus is likely to represent a more advanced level of information processing than the much better studied V1, which is at the lowest level of the hierarchy. Second, V3 receives a direct input from cells in layer 4B of V1 (9, 26, and in preparation). Layer 4B has been shown to be driven largely or exclusively by visual information arising from a subset of retinal ganglion cells ($P\alpha$) and relayed via the magnocellular layers of the lateral geniculate nucleus and layer 4C α of V1 (45). This provides an opportunity to study an area that may be dominated entirely by the functionally distinctive "magnocellular stream". In addition, V3 invites comparison with area MT, which also receives a direct input from cells in layer 4B of V1 and is located at a higher level of the cortical hierarchy. Finally, V3 is unusual in that it contains only a partial representation of the contralateral hemifield. We regard the companion strip adjoining ventral V2 to be a separate visual area, the ventral posterior area, VP. There are several reasons for this distinction, which are discussed in detail elsewhere (9, 76). An important part of the evidence was obtained in the present study, though, and we will return to this issue in the DISCUSSION. Aside from the matter of identifying areas per se, the topic is important from the perspective of understanding the degree to which visual information is processed differently in the upper and lower fields at the same level of the cortical hierarchy.

We have addressed these issues by examining the functional properties of neurons in area V3. We concentrated on investigating neuronal selectivities for orientation, direction, speed, binocular disparity, and color. Some of these (orientation, direction, color) have already been examined in previous qualitatively based studies (5, 81, 90). However, experience has underscored the difficulties in relying on purely subjective assessments of neuronal response properties. Accordingly, we have used quantitative single-unit techniques to investigate the properties of neurons in V3, thereby yielding a reliable basis for comparisons with other cortical areas, particularly VP, which has recently been examined using essentially identical techniques (10). Preliminary accounts of some of these results have previously appeared (9, 23).

METHODS

Animal preparation

The methods employed in the present study are largely similar to those used in previous physiological studies from this laboratory (10, 48, 49). Five cynomolgus macaque monkeys were used for semichronic physiological recordings of neurons in area V3 of extrastriate cortex. Under general anesthesia and sterile conditions, a stainless steel recording chamber was implanted above a craniotomy above cortex that provided access to V3. In general, we approached V3 in a parasagittal plane (1–1.5 cm lateral to the midline) with the electrode aimed ~30° forward from vertical.

Following several days of recovery, we began twice weekly recording sessions. On the day of recording, the animal was anesthetized with ketamine (10 mg/kg im) and placed in a prone position with its head painlessly supported by a custom-designed headholder that eliminated the need for eye or ear bars for support. The monkey was then intubated and respired with a humidified mixture of 75% nitrous oxide and 22.5% oxygen with 2.5% carbon dioxide using a Bird (3M Corp) pressure feedback respirator. Neuromuscular blockade was achieved by injection of gallamine triethiodide Flaxedil (10 mg ip) followed by a continuous infusion of Flaxedil at $7.5 \text{ mg} \cdot \text{kg}^{-1} \cdot \text{h}^{-1}$; ip in 2.5% dextrose and 0.45% saline. The animal's body temperature and EKG were continuously monitored, and body temperature was maintained with a warm-water heating pad.

The eyes were fitted with zero-power contact lenses, and atropine (2%) and Neo-Synephrine (2.5%) were used to achieve mydriasis and cycloplegia. Each eye was brought into focus on the tangent screen (114 cm distant) using trial case lenses as determined by retinoscopy. The positions of the foveas were determined with a reversible ophthalmoscope and were plotted on the tangent screen. Prisms were inserted to superimpose the right and left foveas to within 0.5–1.0°.

A custom designed microdrive, equipped with an adjustable X-Y stage (Central Engineering Services, Caltech) advanced a Paralyene C-coated tungsten microelectrode (Microprobe) through a small hole in the exposed dura. Neural signals were conventionally amplified, filtered, and displayed on an oscilloscope. A window discriminator was used to isolate individual cells and provide a digital input to the computer (PDP 11/34A) corresponding to each isolated action potential. Electrode penetrations were generally marked with one or more strategically placed electrolytic lesions (10 μA for 10 s). At the end of a recording session, the electrode was withdrawn, and the chamber was cleaned with 0.3% H_2O_2 , filled with sterile mineral oil, and sealed with a threaded cap.

Following 8–12 h of paralysis, the infusion of Flaxedil was discontinued and was replaced by an infusion of 5% glucose. Some time later (1–2 h), as spontaneous movements reappeared, recovery was aided by injection of atropine (0.15 mg/kg) followed 10 min later by neostigmine HCl (0.25 mg/kg). Shortly thereafter, normal respiration and muscle tone reappeared and the monkey was returned to its home cage. These twice weekly recording sessions continued for 2–7 wk. At the end of this time, another sterile surgery was performed under general anesthesia. During this procedure, the splenium of the corpus callosum was sectioned and a second recording chamber was usually placed overlying V3 of the left hemisphere.

Visual stimulation and recording procedure

Visual stimuli were provided by an optical projection system that provided manual and computer control over stimulus position, size, orientation, direction, speed, binocular disparity, and color. Narrow-band colors were generated with interference filters and were equated for equal luminance when projected onto a screen of uniform reflectance (10). The projection beam was split so that two slits were projected onto the screen, and their positions and movements were independently controlled by galvanometer-driven mirrors. Except during tests for color selectivity, these two images were differentially plane polarized and projected onto a nondepolarizing screen. Appropriate cross-polarized filters were placed in front of each eye such that each eye only viewed one projected image and two stimuli could be presented with various binocular disparities (13, 49). During tests of color selectivity, the polarizing filters were removed and the two images were brought into alignment.

Once a single unit was isolated, its minimum response field was plotted for each eye and the two plotted fields were aligned using prisms. Field positions and foveal locations were entered into the computer via positional feedback from the galvanometer system. Quantitative testing as described in the text and figure legends then established the unit's spatial and chromatic selectivities. Except where noted, all reported histograms and tuning curves are based on three repetitions of each stimulus parameter presented in pseudo-random order.

Histology

During the terminal recording session, anatomical tracer injections were made into physiologically identified loci in V3 (Ref. 26, and in preparation). Following survival periods of 2–4 days, the monkey was deeply anesthetized with Nembutal and perfused with 0.1 M phosphate buffer followed by buffered 2% paraformaldehyde–0.5% glutaraldehyde. This was followed by either 10% sucrose in the fixative or 10% sucrose in buffer. The brain was

blocked, equilibrated in 30% sucrose, and frozen sections were cut at 31 μ m. Reconstructions of electrode penetrations were made primarily from Nissl-stained sections. The myeloarchitectonic borders of V3 were determined from adjacent sections stain for myelin by a modification of the Gallyas method (32).

RESULTS

Location and identification of V3

Electrode penetrations were directed toward the annectant gyrus (a buried gyrus between the lunate and parietooccipital sulci) and the adjacent lunate sulcus (LS) and parietooccipital sulcus (POS). V3 can be distinguished from neighboring cortex by its distinctive myeloarchitecture (9, 80). Figure 1 illustrates a photomicrograph of a parasagittal brain section, through the annectant gyrus, stained by the Gallyas method for myelin (32). V3 can be recognized by its heavy myelination in layers 4, 5, and 6 as it courses across this buried gyrus. In this photomicrograph, the myeloarchitectonic borders of V3, and the limits of uncertainty of those borders, are indicated by asterisks. In this section, V3 is ~3 mm wide but narrows considerably in more medial and lateral sections in this hemisphere (see Fig. 3).

An electrode penetration that depicts the location of V3 in a parasagittal brain section from a different hemisphere is illustrated in Fig. 2A. In this penetration, receptive fields are drawn for recording site A in V1, B in V2, and sites C–F in V3 (Fig. 2B). As seen in Fig. 2B, receptive fields in V2 were both larger and more eccentric in location than those encountered in V1. The electrode then crossed over to the annectant gyrus, entering V3 near its anteroposterior midpoint as judged by myeloarchitecture (asterisks in Fig. 2A).

The location and full extent of V3 in this hemisphere is best displayed on an unfolded two-dimensional map of extrastriate cortex (see Ref 77). In Fig. 3A, V3 is indicated as a stippled region that extends medially to the parietooccipital sulcus, and laterally across the annectant gyrus, to the fundus of the lunate sulcus. A portion of this unfolded map of extrastriate cortex is reproduced in greater detail in Fig. 3B. Here the myeloarchitectonic borders of V3 are illustrated by thick lines; the limits of uncertainty of those borders are indicated by short lines across the border. The

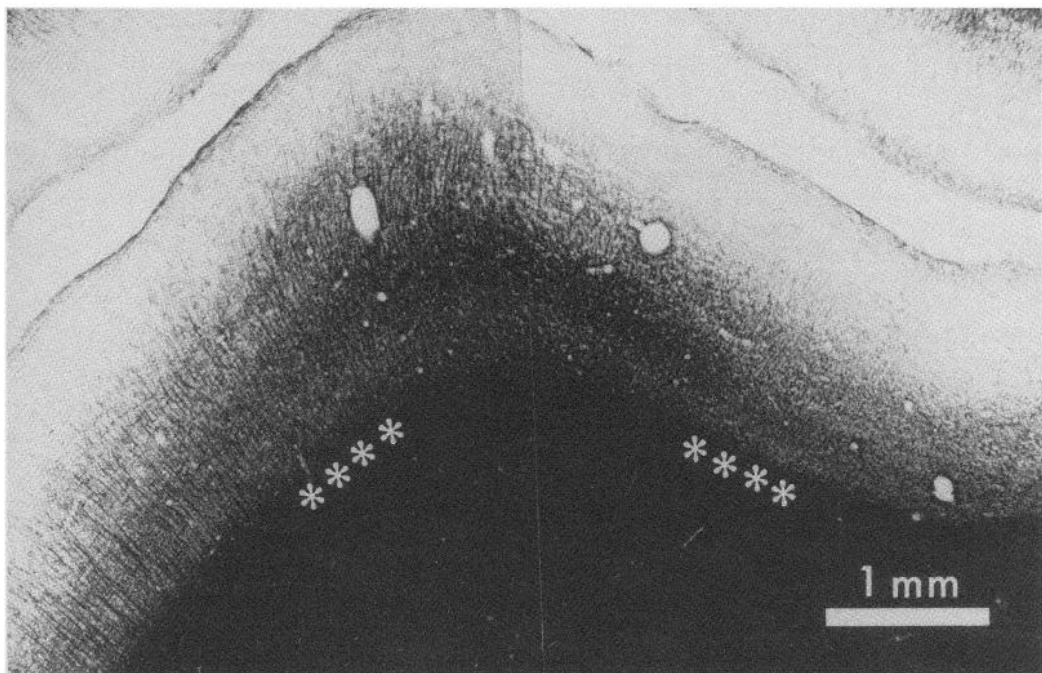


FIG. 1. Photomicrograph of a parasagittal brain section through the annectant gyrus stained by the Gallyas (32) method for myelin. V3 is characterized by dense myelination of layers 6, 5, and 4. The myeloarchitectonic borders of V3 and their uncertainty limits are indicated by asterisks. Anterior is to the left.

contours of layer 4 from selected parasagittal brain sections roughly 2 mm apart are illustrated by continuous thin lines, and the fundus of the lunate sulcus is indicated by a dashed line. In this hemisphere V3 appears as a continuous densely myelinated strip running from near the parietooccipital sulcus to the fundus of the lunate sulcus near the lateral edge of the hemisphere, although myeloarchitectonic discontinuities occur in some other cases (80).

TOPOGRAPHIC ORGANIZATION. The overall pattern of topographic organization in V3 has been examined in several anatomical (80, 84) and physiological (34, 81) studies. Our own recordings confirmed that, in general, central fields are represented laterally and peripheral fields medially in V3. The horizontal meridian is represented along the V2/V3 border and the inferior vertical meridian is represented along the anterior border of V3. This organization is illustrated by a sequence of recording sites starting near the posterior border of V3 and extending anteromedially across the annectant gyrus (Fig. 3B, A-I). The corresponding se-

quence of receptive field locations is illustrated in Fig. 3C. Receptive field positions shift from near the horizontal meridian at $\sim 5^\circ$ of eccentricity (*fields A* and *B*), toward the inferior vertical meridian (*fields E* and *F*). *Receptive fields G-I* were found, as expected, near the inferior vertical meridian at $\sim 10^\circ$ of eccentricity.

From this presentation, one would conclude that V3 has a regular simple topographic organization. However, during the course of these experiments, several examples of disorderly or unexpected topographic progressions were encountered. For example, in one hemisphere, the inferior vertical meridian was represented near the posterior border of V3 as judged by myeloarchitecture. However, other nearby penetrations in this case showed the expected topographic order. In two other cases, the anterior border of V3 was not associated with the representation of the inferior vertical meridian. In one of these, the 45° meridian was represented along the anterior border of V3. In the other, the horizontal meridian was found to be represented anteriorly in V3.

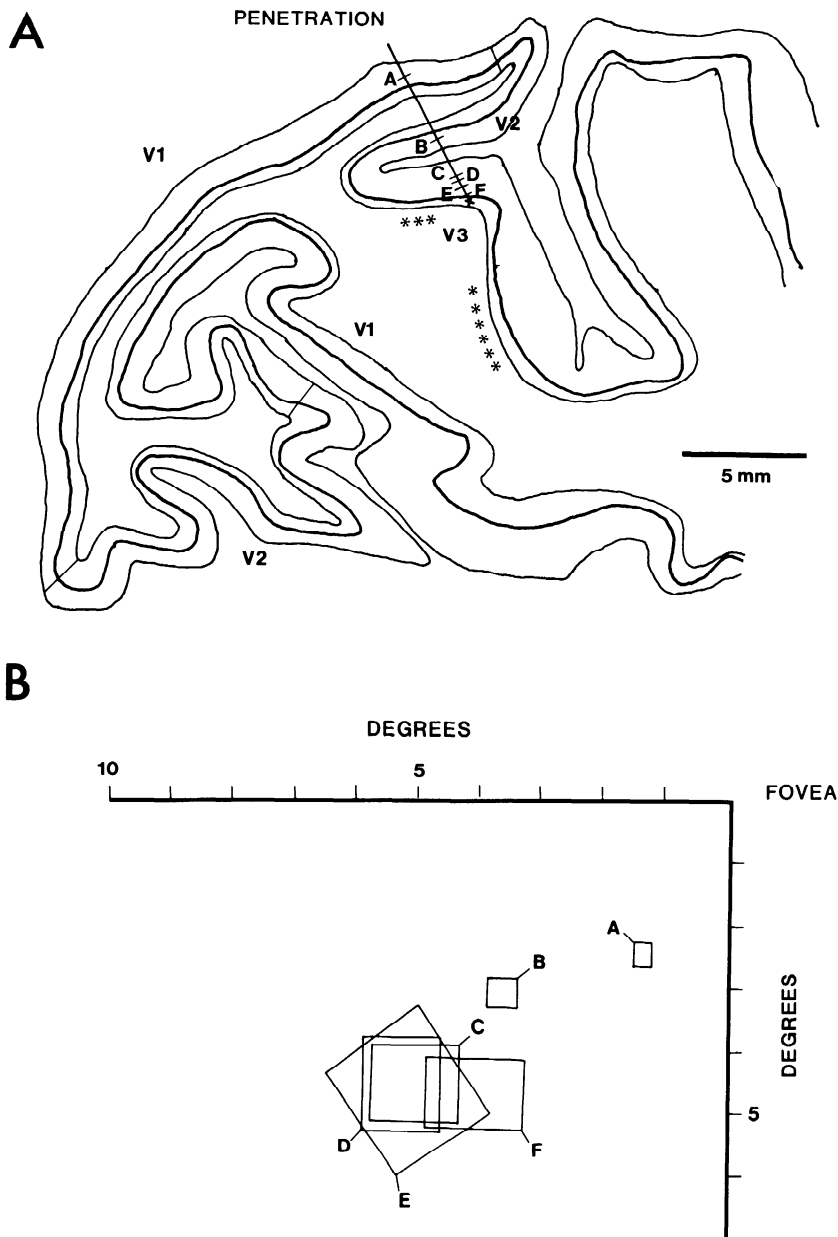


FIG. 2. Location of V3. *A*: parasagittal brain section with electrode penetration entering opercular V1, crossing white matter to enter V2, and crossing the lunate sulcus to enter V3 on the annectant gyrus. Asterisks mark the myeloarchitectonic borders of V3. *B*: receptive field locations encountered in areas V1, V2, and V3 along the penetration illustrated in *A*. Receptive fields in V3 are consistently larger than those encountered in V1 and V2 at comparable eccentricities. Recording site *A* is in V1, *B* is in V2, and *C-F* are in V3.

Based on the topographic organization revealed during these experiments, ~80% of recording sites, within myeloarchitectonic V3, were associated with the expected topographic organization. Pronounced irregularities in topographic organization

organization were thus observed in roughly 20% of V3 recording sites. (These figures include recording sites that provided topographic information but did not provide quantitative information about receptive field

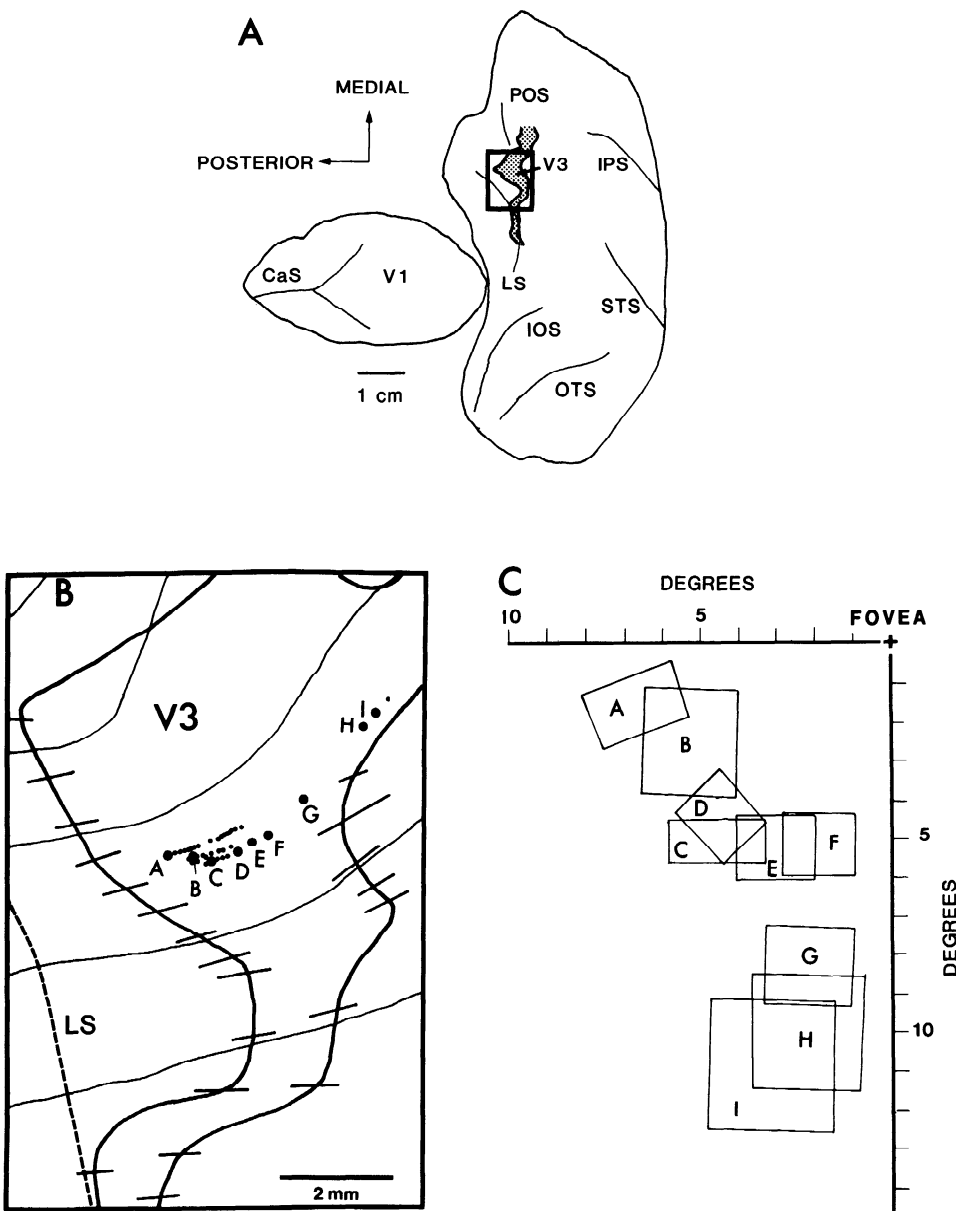


FIG. 3. Topographic organization of V3. *A*: overall two-dimensional map of experimental hemisphere indicating the location of V3 (stippling) in dorsal extrastriate cortex as determined from myeloarchitectonics. *B*: reconstruction of recording sites relative to myeloarchitectonic borders of V3 in an enlargement of a portion of dorsal extrastriate cortex enclosed by the box in *A*. V3 myelin borders are indicated by heavy solid lines and uncertainty limits indicated by short thin lines. Map contours represent layer 4 contours from parasagittal brain sections through the annexant gyrus. A subset of recording sites (*A–I*) highlights the topographic organization of V3. *C*: receptive fields for recording sites *A–I* in V3. Recording sites *A* and *B*, near the posterior border of V3, had receptive fields near the horizontal meridian in the lower field. Receptive field positions shift through the 45° meridian (*sites C and D*) to the near inferior vertical meridian (*sites E and F*). Recording sites *G–I* extend more medially along the anterior border of V3. Receptive fields for these recording sites are more eccentric (8–12°) and are located near the inferior vertical meridian.

properties.) We interpret these results to indicate local topographic complexities within an overall topographically organized visual

area. Finally, these results indicate that topographic organization alone cannot always be used to reliably identify V3 unambiguously,

just as has been found for MT (unpublished observations, 79). Similar evidence for irregularities in V3 topography have been reported by Gattass et al. (34).

RECEPTIVE FIELD SIZE. Receptive fields in V3 were, in general, larger than fields encountered in V1 and V2 at comparable eccentricities. Figure 4 illustrates the relationship between receptive field size and eccentricity (E) for 128 neurons in V3. The best-fitting linear regression for these data is described by receptive field (RF) size (deg) = 0.18E + 1.26. The receptive field sizes encountered in dorsal V2 during these experiments are also illustrated in Fig. 4. Although these V2 receptive fields typically reflect multiunit activity, they were generally smaller in V2 than in V3, but with significant overlap in the distributions. However, the V2 field sizes illustrated here are also smaller than those reported by other investigators (10, 33). It is not clear whether this represents genuine individual variability in different hemispheres, technical differences, such as state of anesthesia, or different criteria for drawing receptive field boundaries used in different laboratories and between different investigators.

The regression slope of 0.18 for our V3 sample indicates a dependence of field size on eccentricity that is comparable to the slope of 0.19 seen in area VP by Burkhalter and Van Essen (10). However, their expression (RF size = 0.19E + 2.96) differs in offset from the present V3 data by an amount that is significant in an analysis of covariance ($F = 186$, $P < 0.0005$). In addition, another investigation of receptive field size in VP (55) derived a steeper slope with less of an offset (VP RF size = 0.32E + 1.32), thus yielding an estimate of field size intermediate between the present study and the Burkhalter and Van Essen study. However, in view of the wide variations found within areas, we do not attach great significance to this V3-VP disparity, especially since no significant field size difference between these regions was found by Gattass et al. (34).

Functional properties

We concentrated our analysis of V3 on the selectivity for the basic parameters of direction, orientation, speed, disparity, and color. In general, individual neurons in V3 showed selectivity for at least one and usually several different stimulus parameters, with the mag-

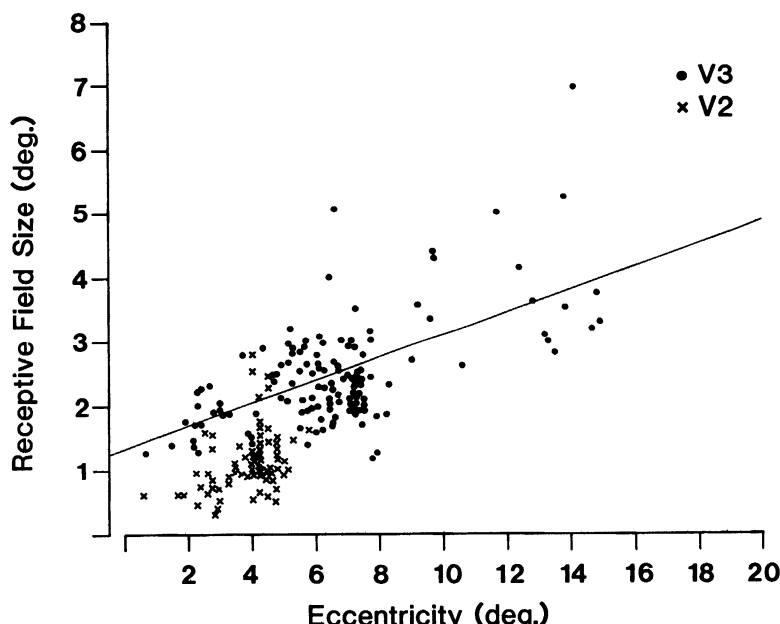


FIG. 4. Receptive field size in V3 and V2. Distribution of receptive field size as a function of eccentricity (E) for 128 neurons in V3 and 71 neurons in V2. Least-squares regression function for V3; RF size (deg) = 0.18(E) + 1.26°.

nitude and types of selectivity varying considerably from one cell to the next.

Figure 5 illustrates the results from one V3 neuron tested for selectivity to stimulus direction, disparity, color, and length. The lower part of panels A-C show a series of poststimulus time (PST) histograms for each parameter

setting; the upper part shows tuning curves based on the mean firing rate, with spontaneous rate of firing shown by dotted lines. This cell showed strong direction selectivity (Fig. 5A), with relatively broad tuning around a peak of 210° (down and to the left). The direction index (DI), calculated as $1 - (\text{null}/$

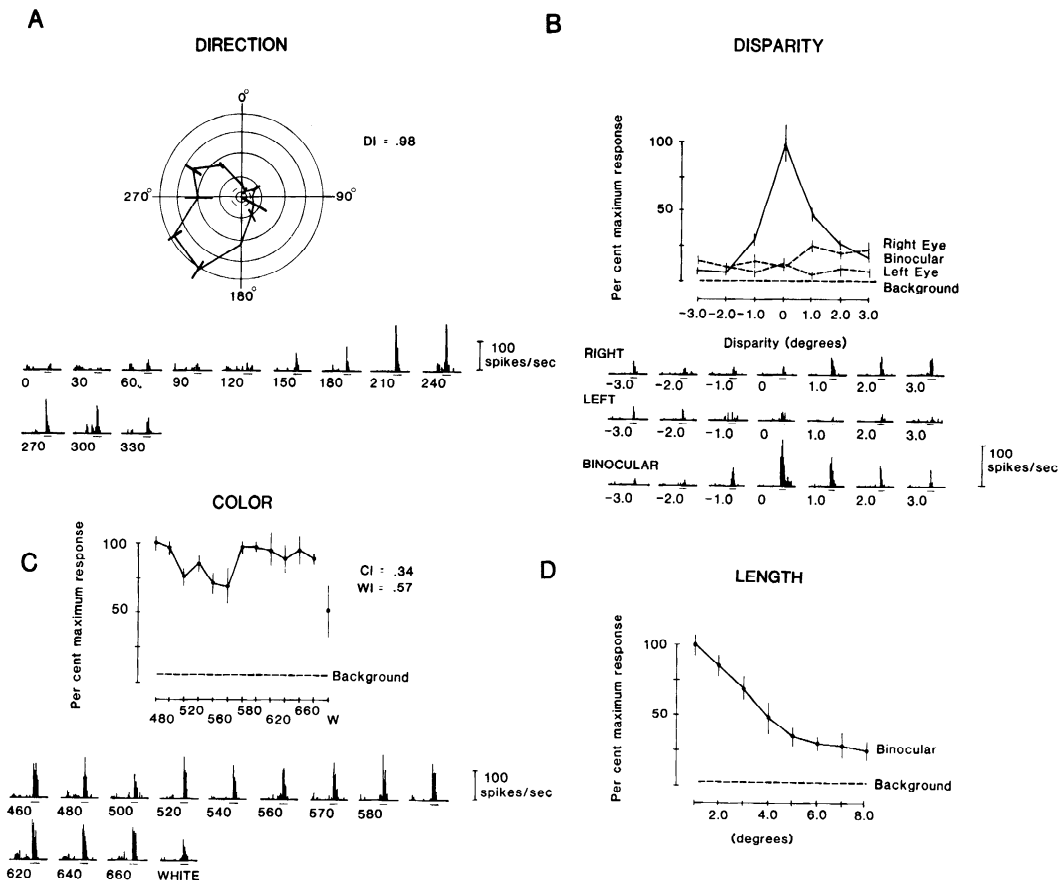


FIG. 5. Tuning profiles for four parameters in a typical V3 neuron. A: polar plot and PST histograms of responses to narrow bar moved through the receptive field in 12 directions separated by 30° . Mean firing rate during movement and standard error of means are indicated. This cell preferred stimuli moving down and to the left and was strongly directionally selective. The direction index (DI) was used to quantify this selectivity and is defined: $\text{DI} = 1 - (\text{opposite direction} - \text{background}) / (\text{best direction} - \text{background})$. Selective cells have high direction indexes near 1 and nonselective cells have low indexes. Values above 1 indicate suppression in the opposite direction. The error bars associated with the average firing rates in this and other panels indicate \pm standard error of the mean. B: disparity tuning tested at 7 fixed disparities. Monocular responses were weak (dotted lines) but binocular stimulation (solid line) showed strong facilitation centered on the plane of fixation and dropped off rapidly in front or behind the plane. Dashed line indicates spontaneous firing level; five stimulus repetitions. C: color selectivity. Responses to 12 narrowband isoluminant colored stimuli and isoluminant white moved through the receptive field in the preferred direction at the preferred speed. This cell gave approximately equal responses to each narrowband color tested and was classified as noncolor selective. The response to white was variable and submaximal. Dashed line indicates background firing level. D: length selectivity. Response as a function of slit length. The maximum response was elicited by the shortest slit tested (1°) and the response dropped off as the slit was lengthened to approach the mapped receptive field border (2.5°). Responses dropped off much more rapidly as the slit encroached on a silent surround. Dashed line indicates spontaneous firing level.

best), was 0.96, indicative of virtually no response in the null direction.

When tested for selectivity to binocular disparity (Fig. 5B), the cell gave weak responses when stimulated through either eye alone (dotted lines) and vigorous responses to binocular stimulation within a restricted range of disparities centered around zero, i.e., at the plane of fixation.

Although this cell was quite selective for stimulus direction, binocular disparity, and speed (not shown), it showed little selectivity for stimulus wavelength (Fig. 5C). Responses to equiluminant monochromatic and white slit stimuli moved through the receptive field are illustrated. This cell responded well to monochromatic stimuli extending from 460 to 660 nm. A color index (CI), analogous to the aforementioned direction index, was used to quantify the response of the least effective monochromatic wavelength relative to the most effective wavelength ($CI = 1 - \text{worst/best}$). This cell had a color index of 0.34. There is a small dip in the tuning curve in the range of 500–560 nm, but we find this variation to be not statistically significant (see RESULTS: COLOR SELECTIVITY). Similarly, a white index (WI = 1 – white/best monochromatic) was used to quantify the response to isoluminant white relative to the most effective monochromatic wavelength. This cell gave a somewhat smaller response to equiluminant white light relative to the narrow-band stimuli and had a white index of 0.57. Although the response to white was highly variable, this difference is statistically significant ($P < 0.05$).

Finally, Fig. 5D is a tuning curve illustrating the selectivity of this neuron for slit length. The cell showed maximum excitation to the shortest bar tested (1°) and showed reduced excitation for all longer bars, including those extending outside the cell's excitatory response field of 1.5° . Thus this cell showed endstopping similar to that described elsewhere in visual cortex (35, 40, 64).

DIRECTION SELECTIVITY. One hundred and forty-seven neurons in V3 were quantitatively tested for their selectivity for the direction of movement. Neurons in V3 were, in general, very responsive to movement of a narrow bar through their receptive fields. They varied greatly, however, in the range of directions to

which they responded. The spectrum included cells that responded well to movement in all directions, bidirectional cells that responded approximately equally well to both directions along the preferred axis but not to the orthogonal axis, and standard direction-selective cells that responded over a narrow range of directions. Finally, a few cells showed a striking complex property of direction selectivity for more than two nonaxial directions.

The degree of selectivity was quantitatively assessed using the DI (see Fig. 5A for details). The distribution of the DI for the sample of 147 V3 neurons is illustrated in Fig. 6A. As indicated earlier, direction selectivity is broadly distributed in V3, with the mean of the distribution of 0.60 ± 0.32 (SD). We have considered three categories of neurons corresponding to direction selective ($DI \geq 0.7$), direction biased ($DI 0.5–0.7$), and nonselective cells ($DI < 0.5$). Given these criteria, $\sim 40\%$ (58/147) of our sample of V3 cells were direction selective and 22% (33/147) were direction biased. The remainder of cells were either bidirectional or nonselective for the direction of movement.

Although the direction-selectivity index provides a measure of a cell's ability to discriminate two opposite directions, it does not describe the narrowness of tuning around the preferred direction. In order to provide a measure of the overall selectivity of V3 neurons to movement, we constructed an average direction-tuning curve for the sample population. This curve, illustrated in Fig. 6B, represents the average response of the 147 V3 neurons to 12 directions of bar movement. This population response curve was generated by normalizing the individual tuning curves to their greatest mean firing rate, aligning all the curves at their preferred direction, and then averaging the curves together. The resultant curve thus illustrates the selectivity of the population of V3 neurons for stimulus motion. Several features of this selectivity are easily recognized from this figure. First, the peak is not rounded, but falls off sharply, indicating that the population is most selective for changes in direction around the preferred direction. Second, although the population as a whole is moderately direction selective ($DI = 0.60$), the minimum responses for the population of cell occurs not in the opposite (null)

direction, but in the vicinity of $\pm 90^\circ$ from the preferred direction. Finally, the tuning curve is nearly symmetrical, and the tuning bandwidth for the population, measured as the half-width at half-maximum response, is $\sim 35^\circ$.

The clustering of cells with similar preferred

directions was investigated by comparing the difference in preferred directions of pairs of direction biased or selective cells separated in cortex by 250 μm or less. Overall, these neuron pairs had similar preferred directions, with a majority of pairs having preferred directions

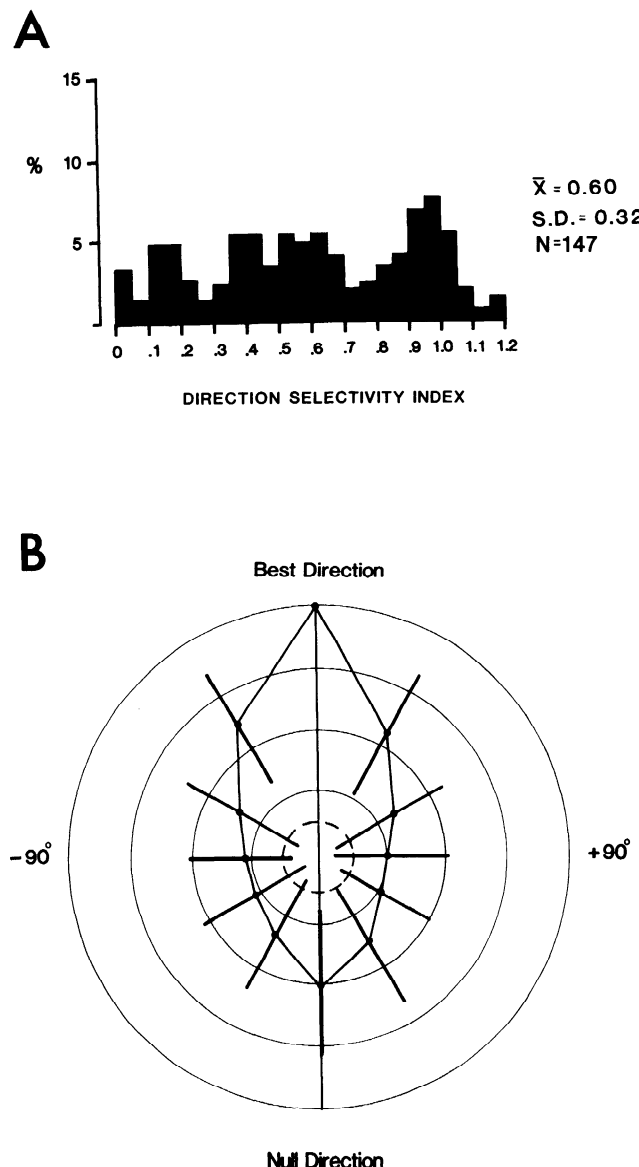


FIG. 6. Direction selectivity in V3. *A*: distribution of the direction index (DI) for 147 neurons in V3. Selectivity for direction varied widely across neurons but a large minority (40%) were strongly direction selective (see text for details). *B*: average direction-tuning curve for the V3 population. Overall, the population response is direction biased ($DI = 0.60$) and the minimum response occurred in the direction orthogonal to the preferred direction. Error bars indicate the standard deviation for each point.

within 30° of one another (35/54; 65%). This clustering of preferred direction is highly statistically significant ($\chi^2 = 59.45$, df = 5, $P \ll 0.001$). In addition, several instances of preferred directions differing by $150\text{--}180^\circ$ were observed (9/54; 17%), but this is not different than would be expected by chance.

ORIENTATION SELECTIVITY. The selectivity for stimulus orientation was quantitatively assessed using both static and moving stimuli. For some cells ($n = 11$) we derived full orientation-tuning curves by examining the responses to flashed bars at six orientations (30° increments). For an additional 14 cells, responses to flashed bars were investigated at only two orientations, parallel to and orthogonal to the best direction of movement. The magnitude of the orientation selectivity in these two groups of cells was expressed by an orientation index (ORI), which is defined as $1 - (\text{response orthogonal to best})/(\text{best response})$. This metric, like the direction index, is near 1.0 for highly selective cells and near 0 for nonoriented cells. The distribution of the orientation index for this sample of 25 V3 neurons is illustrated as the filled histogram in Fig. 7. Overall, the V3 population is strongly orientation selective with an average ORI of 0.88 ± 0.39 (SD). Using the criterion index of 0.7 (best/orthogonal > 3.3), roughly 76% (19/25) of V3 cells were strongly orientation selective.

Orientation selectivity was indirectly assessed in a larger group of cells using the in-

formation contained in the direction series, since this test involved movement of bars of different orientations through the receptive field. To minimize confounding of direction and orientation selectivity, we excluded cells biased or selective along the axis of preferred direction ($DI \geq 0.5$). For the remaining 55 cells, orientation selectivity was assessed by comparing the responses to movement in the preferred direction to the average response to movement along the two directions orthogonal to the preferred. The distribution of the orientation index calculated in response to moving bars is illustrated by the open bars in the histogram of Fig. 7. The average orientation tuning for moving bars (0.84) was essentially the same as for the static orientation tests. In the 10 nondirection-selective cells tested with both methods, the two methods gave nearly identical results for seven cells. However, two cells appeared much more orientation selective to moving bars and one cell was much more orientation selective for stationary stimuli.

SPEED SELECTIVITY. The selectivity for stimulus speed was quantitatively examined in 99 V3 neurons. A bar of qualitatively optimal dimensions was swept through the receptive field of each neuron in the preferred direction at speeds ranging from 0.5 to $128^\circ/\text{s}$. The mean firing rate during stimulus movement was used as the metric to quantify the neuronal response. From these data a speed-tuning curve was derived, and several properties of speed selectivity were calculated, including the pre-

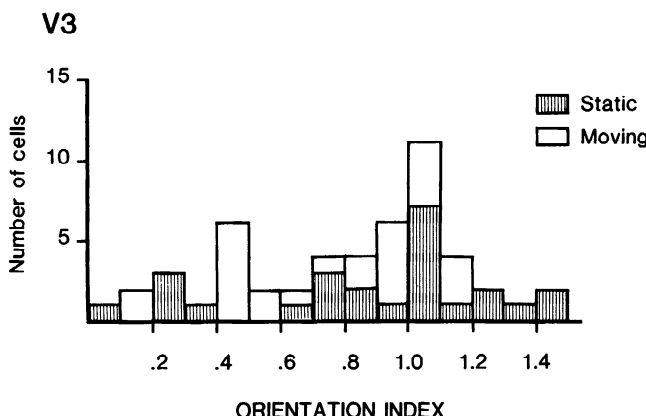
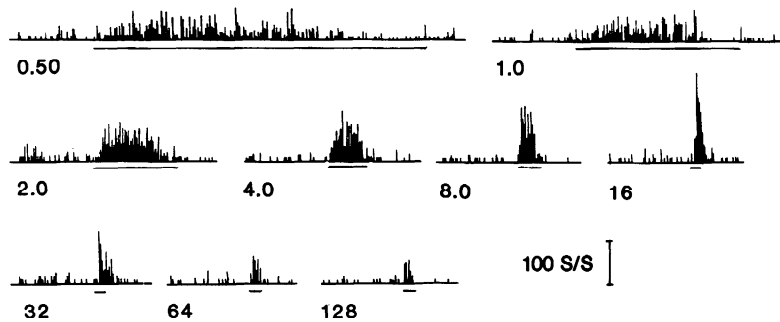
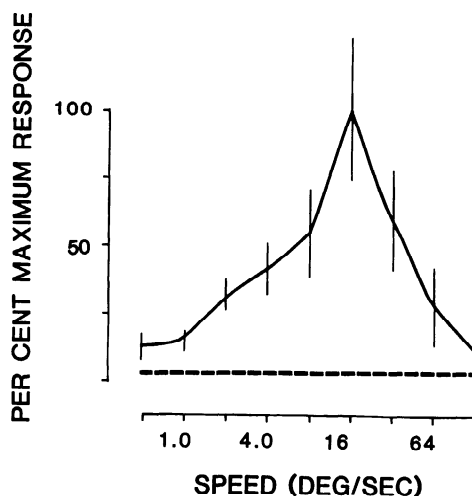
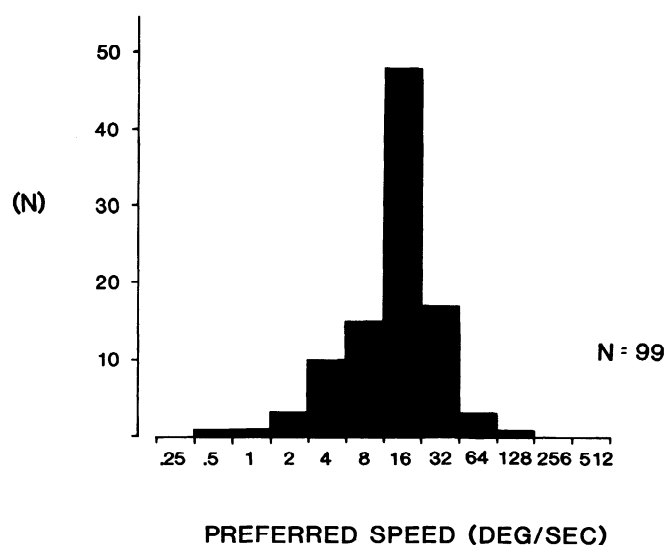


FIG. 7. Orientation selectivity in V3. Distribution of the orientation index for the V3 population. The *filled histogram* indicates orientation index determined from flashed bars, *open histogram* from moving bars (see text for details). Overall, neurons in V3 are highly orientation selective. Nonoverlapping entries (cf. Ref. 10).

A**B**

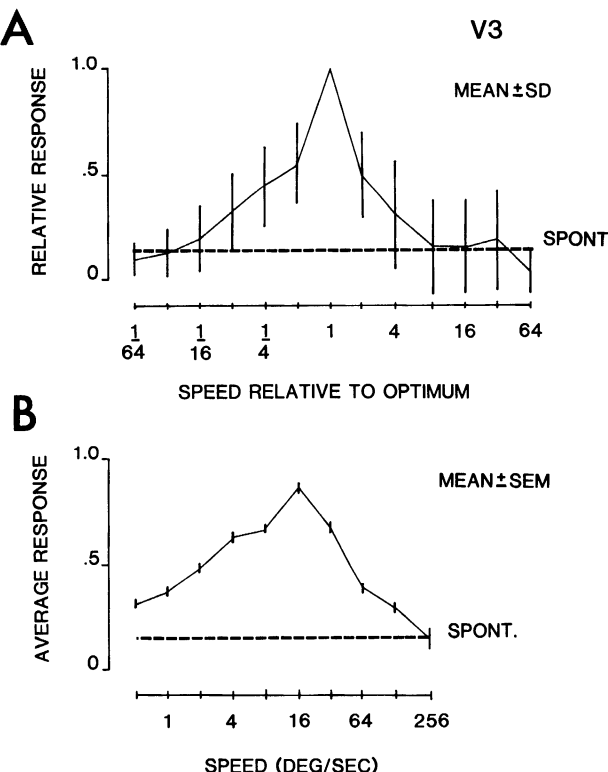


FIG. 9. *A*: relative speed tuning in V3. This curve illustrates the tuning of 99 V3 cells for speed relative to their preferred speeds. This curve was generated by normalized individual tuning curves, aligning them at their preferred speed, and averaging them together. *B*: average V3 population response to stimuli moving at different speeds. Individual speed-tuning curves were normalized and averaged together. The maximum population response occurs for stimuli moving at $16^{\circ}/s$. Dashed line indicates spontaneous firing level.

ferred speed and tuning bandwidth. Ninety percent (89/99) of the cells tested were clearly tuned for speed in that their tuning curves fell by 50% at speeds both faster and slower than optimum. Seven other cells (7/99; 7%) were considered marginally tuned in that the response did not quite drop by 50% on one side of the peak. Finally, three cells (3/99; 3%) did not appear obviously tuned for speed in that they continued to give brisk responses to the fastest speeds tested. Figure 8*A* illustrates the PST histograms and resultant speed-tuning curve from a typical V3 neuron. This cell responded most vigorously to moderate speeds ($16^{\circ}/s$), but gave at least a weak response to a

wide range of speeds. Most speed-tuning curves in V3 were of similar shape, with the responses dropping off more rapidly on the high-speed side of the curve than on the low-speed side (note semilog plot). The distribution of preferred speeds sampled in V3 is illustrated in Fig. 8*B*. Nearly half of the cells are tuned to a speed of $16^{\circ}/s$, and 81% (80/99) had optima between 8 and $32^{\circ}/s$.

An average speed-tuning curve for V3 neurons was generated by normalizing individual tuning curves, aligning the curves at their preferred speed, and averaging the remaining points. The resultant relative tuning curve (Fig. 9*A*) is sharp around the preferred speed, thus

FIG. 8. Speed selectivity in V3. *A*: PST histograms and speed-tuning curve of a typical V3 neuron. A narrow slit was moved through the receptive field in the preferred direction at 9 speeds ranging from 0.5 to $128^{\circ}/s$. This cell preferred stimuli moving at $16^{\circ}/s$. *B*: distribution of preferred speed for 99 V3 neurons. Most cells preferred stimuli moving at $16^{\circ}/s$ and few cells preferred speeds faster or slower by more than a factor of two.

indicating a maximum speed selectivity near the best speed. The full tuning width at half-maximal response corresponds to a 4.4-fold change in speed. In addition, this relative tuning curve is slightly asymmetrical and is characterized by a more rapid decrease in response for speeds faster than the preferred than for slower speeds.

The overall response of the population of V3 neurons to stimuli moving at different speeds is illustrated in Fig. 9B. This curve was generated by normalizing individual speed-tuning curves and averaging them together without shifting their peaks. The peak population response occurs at a speed of $16^{\circ}/\text{s}$, as expected from the distribution of optimal speeds in Fig. 8B. Once again, the curve is asymmetrical in that the responses diminish more rapidly to the right than to the left of the peak. The overall response curve is rather broad, though; as a population, responses of half-maximal or greater response rates were observed over the range from 4 to just over $32^{\circ}/\text{s}$.

MULTIPEAK ORIENTATION AND DIRECTION SELECTIVITY. The vast majority of neurons encountered in V3 showed simple orientation-and/or direction-tuning properties much like that reported in lower visual areas. A few cells in our sample, however, showed significantly more complex response profiles. Figure 10 illustrates the responses from two such cells, including orientation and direction data from one cell (*A*, *B*) and orientation data from another cell (*C*). First considering orientation selectivity, the cell in 10*A* gave a good response to a vertically oriented bar flashed on in its receptive field. The cell was very tightly tuned for this axis, with no response to a flashed bar 30° from optimal. However, when the bar was oriented at 60° from vertical, a second, sharply tuned response peak was found. A similar example is seen in Fig. 10C. This cell gave good responses over a 30° range near vertical, a second peak at an orientation of $45-60^{\circ}$, with no responses at any intermediate orientations.

Similar multipeaked responses were found in several cells tested with moving bars. For example, Fig. 10B shows results of a directionality test from the same cell as in 10A. This cell gave tightly tuned responses in two nonaxial directions. One peak, at a direction of 150° , was orthogonal to the 60° peak in the orientation series; the second peak, at a

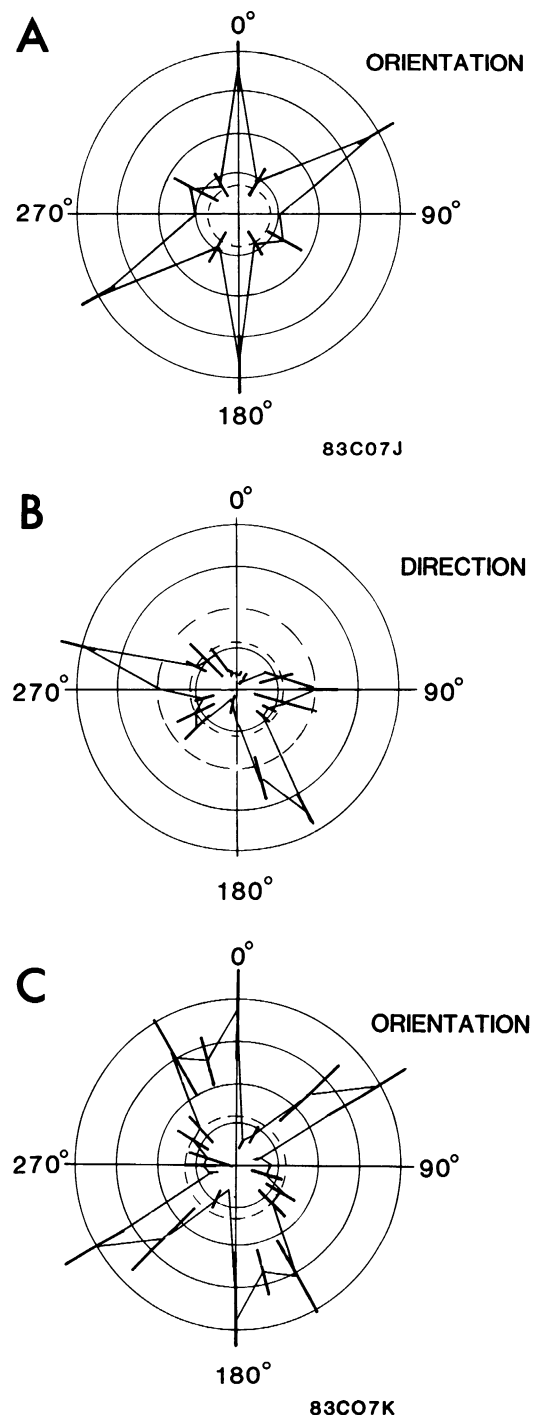


FIG. 10. Multipeaked orientation and direction selectivity. *A*: polar plots of orientation data from 2 cells that showed tightly tuned responses to more than one orientation. *B*: polar plot of responses to moving bar in the same cell as *A*. This cell also gave tightly tuned responses to bar movement in 2 nonaxial directions. *C*: multipeaked orientation tuning as in *A*. Dashed line indicates spontaneous firing level. Five stimulus repetitions in *C*.

direction of 285°, was nearly orthogonal to the orientation peak at 0°. The fact that this cell was unidirectional along each axis of orientation suggests that it might be involved in processing a complex type of motion information, such as determining the direction of real object motion rather than simply that of a single edge (see DISCUSSION).

Perhaps the most striking example of multipeaked direction selectively is illustrated by the cell in Fig. 11A. This cell was selective for three nonaxial directions of movement, separated by angles of ~90, 120, and 150°. The tuning around each of these directions was impressively narrow, in that practically no response was observed for directions just 30° on either side of each peak.

Three other cells in our sample showed unambiguously multiple, nonaxial peaks. Two

of them (Fig. 11, B and C) showed only two peaks, 90° apart for one and 120° for the other. The third (Fig. 11D) showed three peaks, at angles of 60 and 120° apart.

Five of the 10 multidirection/multiorientation cells encountered in this study occurred in a single cluster from one penetration. The remaining multipeak cells occurred as isolated examples. Aside from a suggestion of anatomical clustering, there is little else we can infer from our small sample about the spatial distribution of such cells.

DISPARITY SELECTIVITY. During manual plotting, most cells gave strong, roughly balanced responses when tested through either eye alone. Other cells gave weak monocular responses but showed strong binocular facilitation. Disparity selectivity was quantitatively

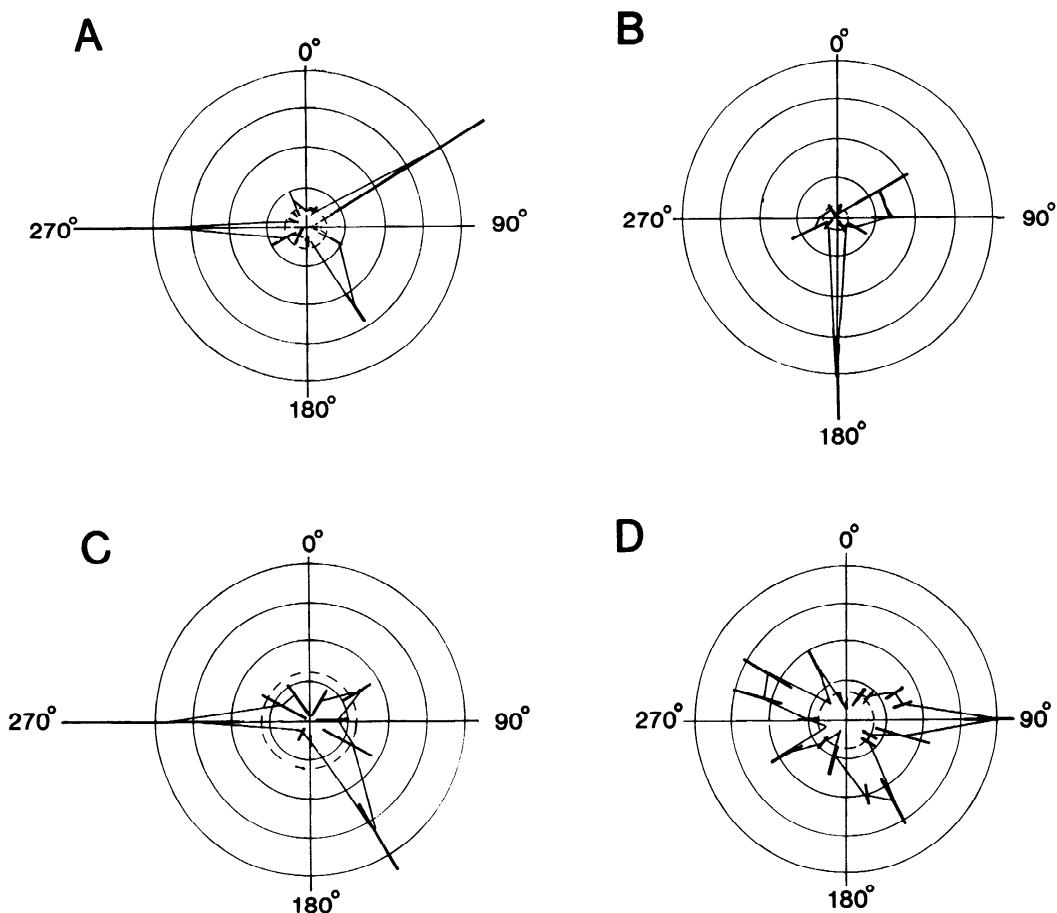
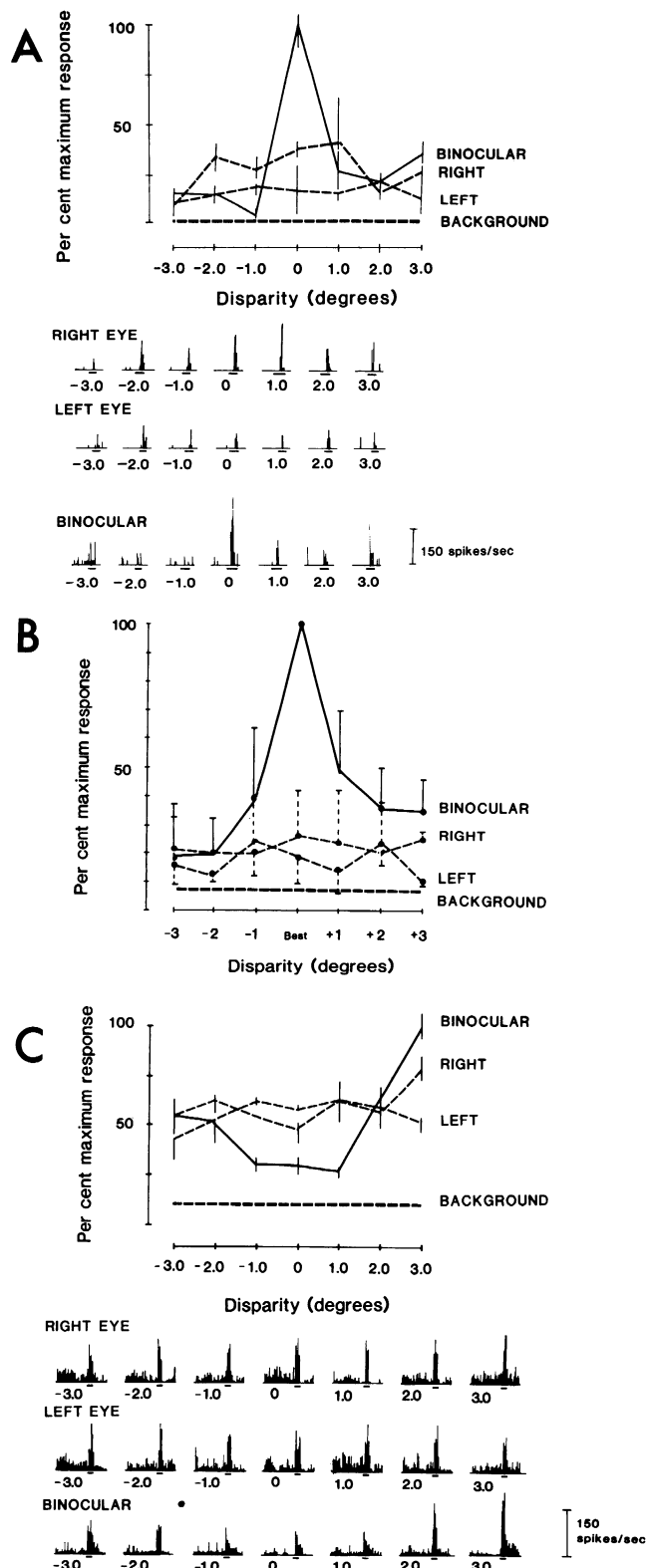


FIG. 11. Complex direction selectivity. Polar plots of responses in four V3 cells to a single bar moved through their receptive fields. Each cell gave tightly tuned responses at 2 or more nonaxial directions. Cells have been ranked according to the clarity of their complex direction tuning. Five stimulus repetitions in D.



tested by presenting moving stimuli typically over a range of 3° in front and behind the plane of fixation.

The most commonly encountered type of disparity selectivity is illustrated in Fig. 12A. This cell gave weak responses when stimulated through either eye alone, but gave a vigorous response when tested binocularly with zero disparity (at the plane of fixation). This peak response dropped off markedly within 1° of crossed or uncrossed disparity. This type of binocular interaction has been termed tuned excitatory (see Ref. 60) and was observed in 28% (13/46) of the sample tested for disparity tuning. The average disparity-tuning curve for this group of tuned excitatory neurons is illustrated in Fig. 12B. It should be noted that there was generally a $\pm 0.5^\circ$ uncertainty in the plots of each fovea so we cannot exclude the possibility of binocular facilitation peaking off the plane of fixation. The average tuning curve was generated by aligning the peaks of individual curves before averaging. This curve, like the individual tuning curve in 12A, shows weak monocular responses from either eye and a strong binocular interaction that is maximal at zero disparity. The population response is most sensitive to deviations around the plane of fixation, and the average response drops off by $\sim 50\%$ for deviations of 1° from zero disparity.

Another group, encountered less frequently (7/46; 15%), showed selectivity for binocular disparity that either was asymmetrical around the plane of fixation or had broadly tuned inhibition around zero disparity. PST histograms and the resultant tuning curve from one such cell is illustrated in Fig. 12C. This cell gave relatively strong monocular responses through either eye, but its binocular response was facilitated at $+3^\circ$ of disparity and was inhibited over a broad range from -1 to $+1^\circ$ of disparity. A few cells showed asymmetric tuning

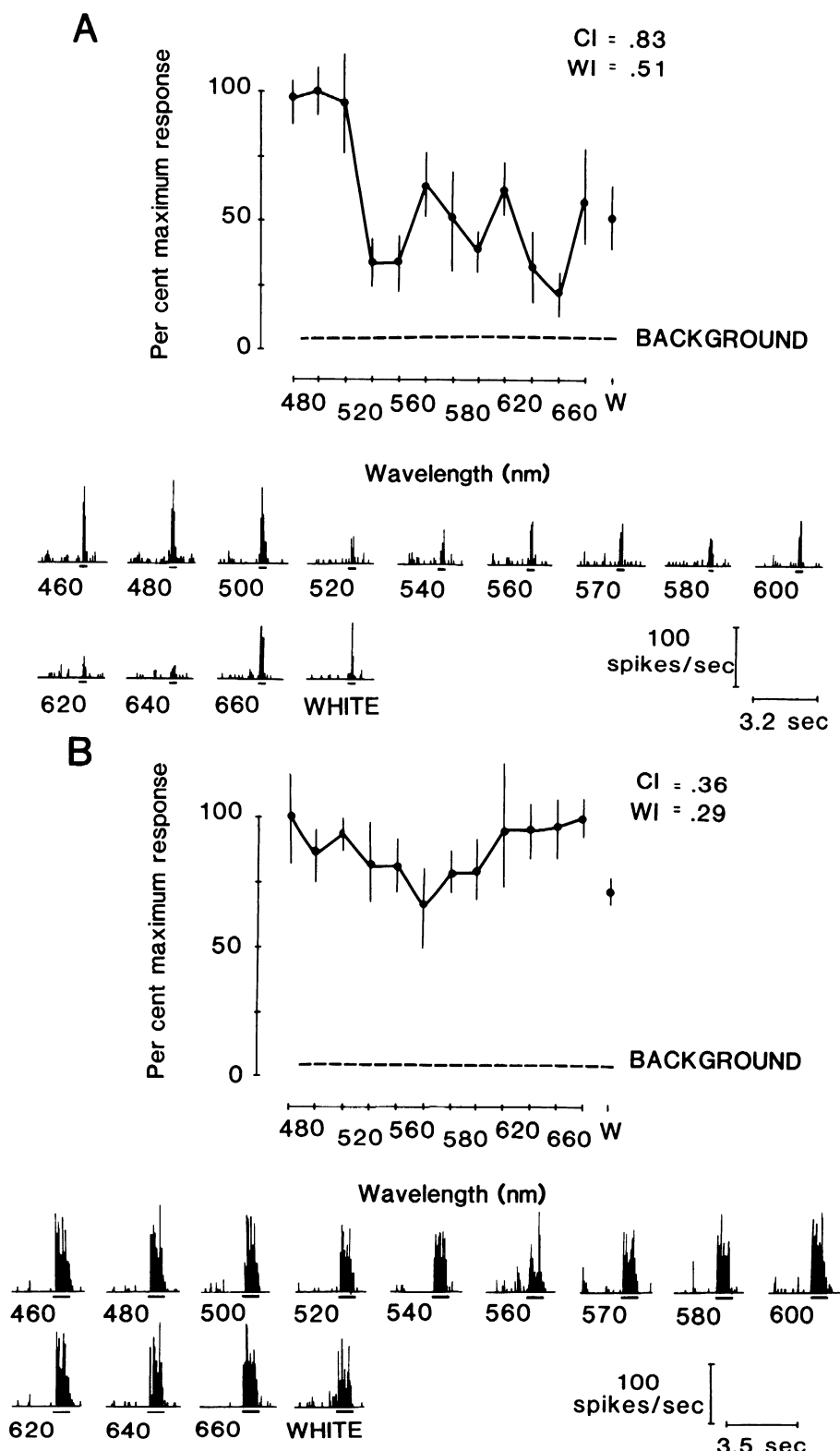
curves suggestive of "near" or "far" cells (60), but the number of such cells did not warrant further subdivision of this group. Finally, about half of the V3 cells tested (26/46; 57%) were not demonstrably selective for binocular disparity; these cells generally gave monocular responses comparable to the binocular response.

COLOR SELECTIVITY. Color selectivity was assessed by examining the relative responses of an individual neuron to a range of monochromatic and white stimuli all matched for their photopic luminance. In most cases, a qualitatively determined optimal size bar was moved through the receptive field at the quantitatively determined best direction and speed. To quantitate the color selectivity of each cell, we used several approaches.

The first two utilized a pair of indexes identical to those used in a study of VP (10). A color index (CI, see legend to Fig. 13) compared the magnitude of response to the least effective wavelength with the most effective wavelength amongst all monochromatic stimuli tested. This index, like others already discussed, yielded values near 1 for highly selective cells and values near 0 for completely nonselective cells. A separate index was also employed to express the relative response to white light. The white index (WI, see legend to Fig. 13) compared the response to photopically matched white light with that to the best monochromatic stimulus. The white index was computed in a way that gave high values for cells unresponsive to white (i.e., selective for some wavelength over white) and low values for cells as responsive to white as to the best monochromatic wavelength.

Contrary to previous reports (5, 81, 90), a significant proportion of cells in V3 showed genuine selectivity for stimulus color. PST histograms and the corresponding tuning

FIG. 12. Disparity tuning in V3. *A:* PST histograms and disparity tuning curve for a tuned excitatory neuron. Monocular stimulation produced minimal responses, whereas binocular stimulation was associated with tuned facilitation, which peaked at the plane of fixation. Three-degree sweeps, three repetitions. *B:* average disparity tuning curve for 13 tuned excitatory neurons in V3. Disparity selectivity was indicated by a greater than 3:1 difference in mean firing rate across the tested range of disparities. Only those cells that showed smooth variations across changes in disparity were included in these analyses. Tuned excitatory cells were selected on the basis of tuning curve shape. *C:* PST histograms and disparity tuning curve for a tuned inhibitory V3 neuron. Monocular stimulation through either eye produced moderate responses. Binocular stimulation produced responses that varied in magnitude as a function of disparity. The minimum response was associated with binocular stimulation at the fixation plane ($\pm 1^\circ$) and maximum excitation was associated with 3° of crossed disparity. Four-degree sweeps, three repetitions.



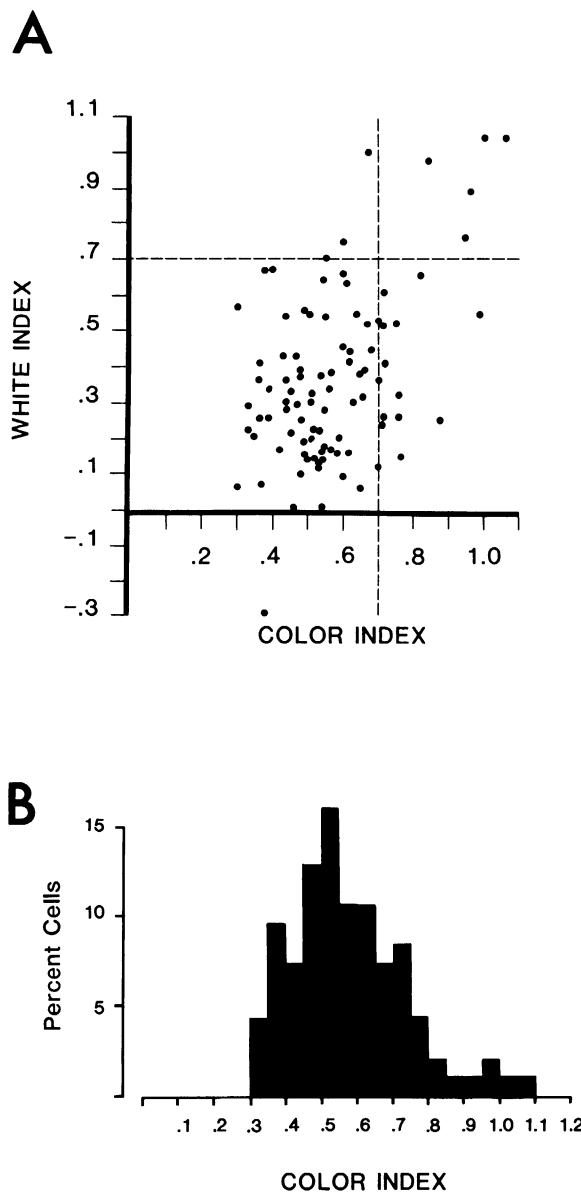


FIG. 14. *A*: joint distribution of color and white indexes in V3. Cells varied continuously in their selectivity for color and their responsivity to white. Dashed lines indicate criterion limits for color-selective and white suppressed cells. *B*: distribution of the color index of 94 V3 neurons. Cells varied widely in their color indexes. Twenty-one percent of the cells had color indexes ≥ 0.7 and thus were classified as color selective (see text for details).

FIG. 13. Color selectivity in V3. *A*: PST histograms and color-tuning curve from a color-selective V3 neuron. Twelve isoluminant narrowband slit stimuli and isoluminant white were moved through the receptive field in the preferred direction at the preferred speed. Dashed line indicates the spontaneous firing level. The magnitude of the selectivity for color was quantified using the color index (CI) and is defined: $CI = 1 - (\text{response to least effective monochromatic wavelength} - \text{background}) / (\text{response to most effective monochromatic wavelength} - \text{background})$. The responsivity to isoluminant white was quantified using the white index (WI) and is defined: $WI = 1 - (\text{response to white} - \text{background}) / (\text{response to most effective monochromatic wavelength} - \text{background})$. High white indexes indicate a submaximal response to isoluminant white stimuli. *B*: PST histograms and tuning curve from a non-color-selective V3 neuron. Same stimuli as used in *A*.

curve from a color-selective V3 neuron are illustrated in Fig. 13A. This neuron was maximally excited by short-wavelength stimuli and had a weaker response to middle and long wavelengths and to white. The cell in Fig. 13A shows good color selectivity. Its color index was 0.83, well above the cut-off level of 0.7 that we previously suggested (76) to be a reasonable criterion for classifying a cell as color selective (9, 10).

The majority of cells in V3 gave similar responses across the visible spectrum; an example of such a nonselective cell is illustrated in Fig. 13B. The response to even the least effective stimulus was vigorous (at least 60% of the maximum); color and white indexes were 0.36 and 0.29, respectively.

In order to determine whether clearly defined classes could be defined on the basis of one or two color-related measures, we plotted in Fig. 14A the joint distribution of the color index (abscissa) and white index (ordinate) for the whole V3 population. From this plot, it is evident that both indexes vary continuously within the population, with no clear evidence

for distinctly clustered subpopulations. Using the same criterion level of 0.7 for the color index as was used for the direction index, 21% (20/94) of the V3 sample was color selective. This group can be further subdivided on the basis of the white index into five color-opponent cells ($WI > 0.7$) and 15 color-biased cells ($WI < 0.7$).

A histogram of just the color index for the sampled V3 population (Fig. 14B) shows a clearly unimodal distribution with a mean of 0.57 and a range of 0.3–1.1. The absence of cells with a color index below 0.3 is related to the inherent variability in the responses to equipotent stimuli. A cell having no color selectivity and no response variability would, of course, have a color index of exactly zero. However, with the variability typical of extrastriate neurons (as evidenced by the size of the standard errors of the mean shown in preceding figures) it is predictable that with only three to five repetitions of each stimulus there would generally be substantial differences between maximal and minimal responses to 12 different wavelengths.

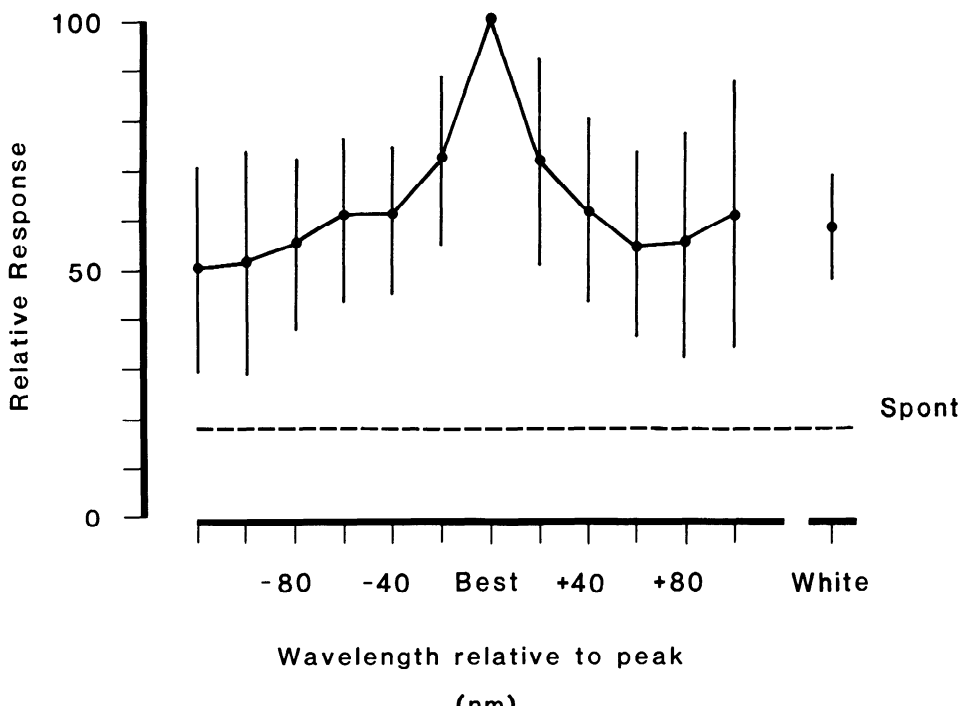


FIG. 15. Average color tuning in V3. Tuning curves from the 20 color-selective cells in V3 were normalized, aligned at their preferred wavelengths, and averaged together. The average color-tuning curve is rather narrowly tuned with a half-width at half-amplitude of ~50 nm.

TABLE 1. *Multiple selectivities of V3 neurons*

Fraction Of (%) Cells Selective For:	Orientation	Direction	Disparity	Color
All	76 (61/80)	40 (58/147)	43 (20/46)	21 (20/94)
Orientation selective		40 (8/18)	44 (7/16)	33 (14/42)
Direction selective	90 (9/10)		53 (9/17)	30 (12/30)
Disparity selective	89 (8/9)	39 (9/23)		20 (4/20)
Color selective	93 (14/15)	48 (13/27)	40 (4/10)	

Percentage incidences of selectivities (with numbers of cells indicated in parentheses) are shown for different parameters by all cells and separate subpopulations. Selectivity for each parameter was quantitatively assessed (see text for details).

Although color-selective cells were relatively rare in V3, we were interested in whether their sharpness of tuning is comparable to that seen in other cortical areas where color-selective cells are more prevalent. To this end, an average color-tuning curve for the 20 color-selective cells in V3 was constructed by normalizing the individual color-tuning curves, aligning them at their preferred wavelength, and averaging the curves together (Fig. 15). Several points can be made from this average color-tuning curve. First, the maximum selectivity for color occurs around the preferred wavelength for the aggregate population, although this was not always the case (e.g., Fig. 13A). Second, the average response drops to a plateau of about half the peak response, indicating a general lack of strong color opponency from antagonistic cone inputs even amongst this subpopulation. Finally, the narrowness of this average color-tuning curve was described by a full bandwidth at half maximum response above background of ~80–100 nm.

MULTIPLE SELECTIVITIES OF SINGLE CELLS. Given that most cells were tested for selectivity to at least two parameters and often three or four, we were able to compare the incidence of multiple selectivities in single cells. We were specifically interested in whether the incidence of one type of selectivity (e.g., orientation) affected the probability that a cell was also selective for other parameters. Burkhalter and Van Essen (10) found the incidence of each type of selectivity in VP to be largely independent of other types of selectivities. V3, with a different cross section of individual selectivities, offers an independent test of this issue. Table 1 illustrates the properties of the whole population and various subpopulations of cells

that show specific stimulus selectivities. For example, orientation selectivity was observed in 76% of all cells tested and was marginally more prevalent in the subpopulations of direction, disparity, or color selective cells (90%, 89%, 83%). Direction selectivity was observed in 40% of the V3 population as a whole, and at approximately the same frequency in the various subpopulations (orientation: 40%; disparity: 39%; color: 48%). The selectivity for binocular disparity and color also appeared comparably prevalent in the whole population and each subpopulation. These results suggest that selectivity for each stimulus parameter is independent of other selectivities and follows the proportions of the population as a whole. Thus neurons follow the same trends for multiple selectivities as were observed in VP neurons (10). Data such as these argue against separate “channels” through areas V3 or VP, where as a similar type of analysis for V2 suggests that two or more separate “streams” co-exist in different compartments of V2 (18, 70).

DISCUSSION

We have confirmed previous reports (5, 81, 89) that many neurons in V3 are selective for orientation and in addition have shown selectivity for direction, speed, and binocular disparity, which previously had not been tested systematically in V3. We found a greater incidence of direction selectivity than previously suspected and, contrary to previous reports, we demonstrated a small, but significant, incidence of color selectivity in V3. All of these basic properties are already present in antecedent cortical areas (V1 and V2). Moreover, these selectivities, in general, do not become sharper in V3 or, for that matter, in other higher cortical areas (cf. Ref. 76). Cells in V3,

like many other cortical neurons, are generally selective for more than one stimulus dimension. This implies that V3 neurons are not simple unidimensional "feature detectors." Instead, they respond differently over a relatively broad portion of a multidimensional parameter space. Therefore, individual V3 cells provide fundamentally ambiguous information about any particular stimulus attribute, and in this important respect they are like cells in all other topographically organized cortical areas studied to date (76, see also Ref. 7). Obviously, comparisons within a population of neurons having overlapping response spaces are needed to resolve such ambiguities, but the nature of where and how these comparisons are implemented in the brain remains a major enigma.

Functional streams in visual cortex

In order to assess the role V3 may play in visual information processing, it is useful to compare the present findings with those from other visual cortical areas. To begin, we review briefly the evidence for distinct functional streams associated with the magnocellular and parvocellular layers of the lateral geniculate nucleus (LGN). As illustrated schematically in Fig. 16, the magnocellular stream (hatched entries) contains eight identifiable processing stages, beginning in the retina with the population of large $P\alpha$ -cells that constitute a small minority of retinal ganglion cells. Their outputs are relayed by way of the magnocellular LGN layers and layer 4C α of V1 to layer 4B of V1. Its outputs are then sent to extrastriate areas V3, MT, and part of V2, probably the thick cytochrome oxidase stripes (Ref. 26, 50, 80). From here, magnocellular-derived information is directed toward several subdivisions of the parietal lobe including the medial superior temporal area and the ventral intraparietal area. The parvocellular stream contains a comparable number of identified stages, beginning with the $P\beta$ -cells, which form the predominant retinal ganglion cell type. Their outputs are relayed by way of the parvocellular LGN layers to layers 4C β and 4A of V1 and from there to the superficial layers of V1 (probably including both cytochrome oxidase-rich blobs and interblobs). The blobs and interblobs project to thin cytochrome oxidase stripes and the interstripes in V2, respectively,

which in turn project to area V4 (18, 44, 70). Finally, this parvocellular-derived information is routed toward several subdivisions of inferotemporal cortex (e.g., 25, 27, 63, 68). It is important to point out, however, that this segregation of the magnocellular and parvocellular streams is not absolute. For example, V3 has strong connections with V4, indicating a magnocellular contribution to the parvocellular stream heading to the temporal lobe (26).

Physiologically, there are several striking distinctions between magnocellular and parvocellular streams in the retinogeniculostriate portion of the visual pathway. Cells in the magnocellular stream are characterized by a lack of color selectivity, transient responses to flashed stimuli, fast conduction velocity, relatively large receptive fields, and activation by low contrast stimuli (e.g., 8, 14, 15, 20, 21, 43, 73, 82). In addition, the majority of cells in layer 4B of V1 are direction selective (19). In contrast, cells in the parvocellular stream are characterized by a high incidence of color selectivity, sustained responses to flashed stimuli, slower conduction velocity, relatively small receptive fields, and poor responses to low contrast stimuli (e.g., 8, 14, 15, 20, 21, 43, 73, 82). On the other hand, there are some prominent receptive fields properties, such as orientation selectivity and disparity selectivity, which are common in both magnocellular-dominated and parvocellular-dominated layers of V1 and which therefore do not provide a strong basis for discrimination between streams (41, 46, 60).

In order to facilitate comparisons of physiological properties in V3 versus that in other various cortical areas, we have compiled the results of all published studies giving numerical estimates of the incidence of selectivity for stimulus orientation, direction, disparity, and color (Fig. 17). Each entry is indicated by a closed circle if the testing of the particular type of selectivity was done using quantitative measures of neural responses and by an open circle if the testing was done using subjective estimates. Numbers alongside each entry denote the particular study, as encoded in the figure legend.

ORIENTATION. Our estimate of orientation selectivity in V3 (76%) is in good agreement

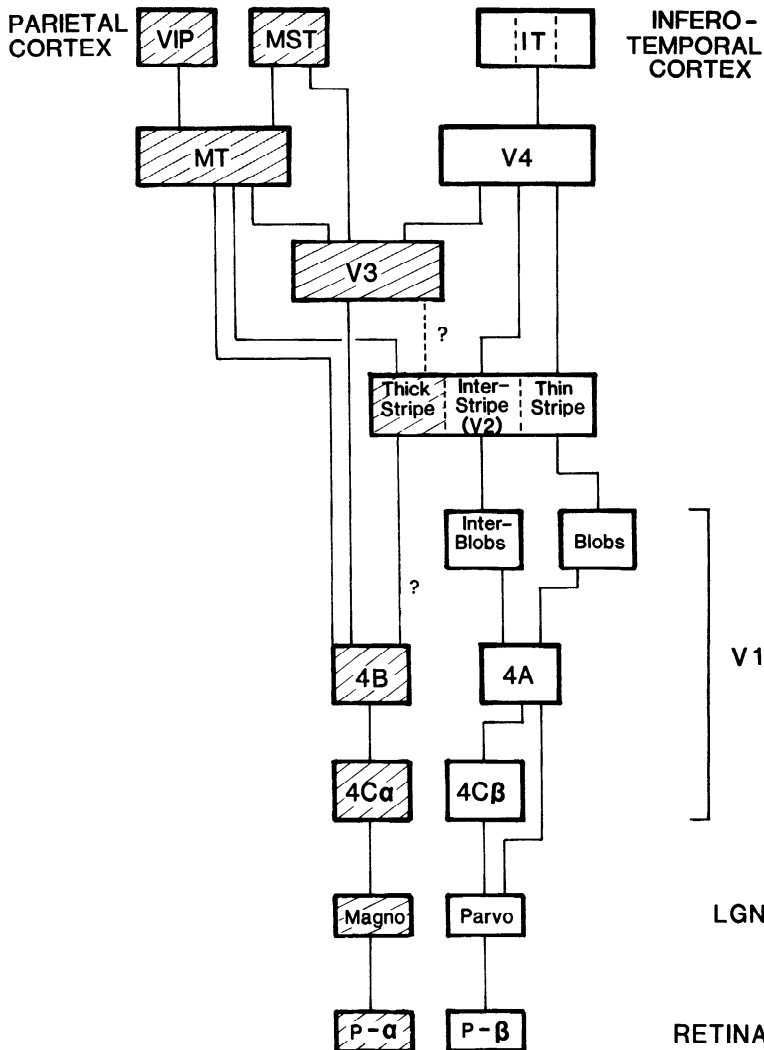
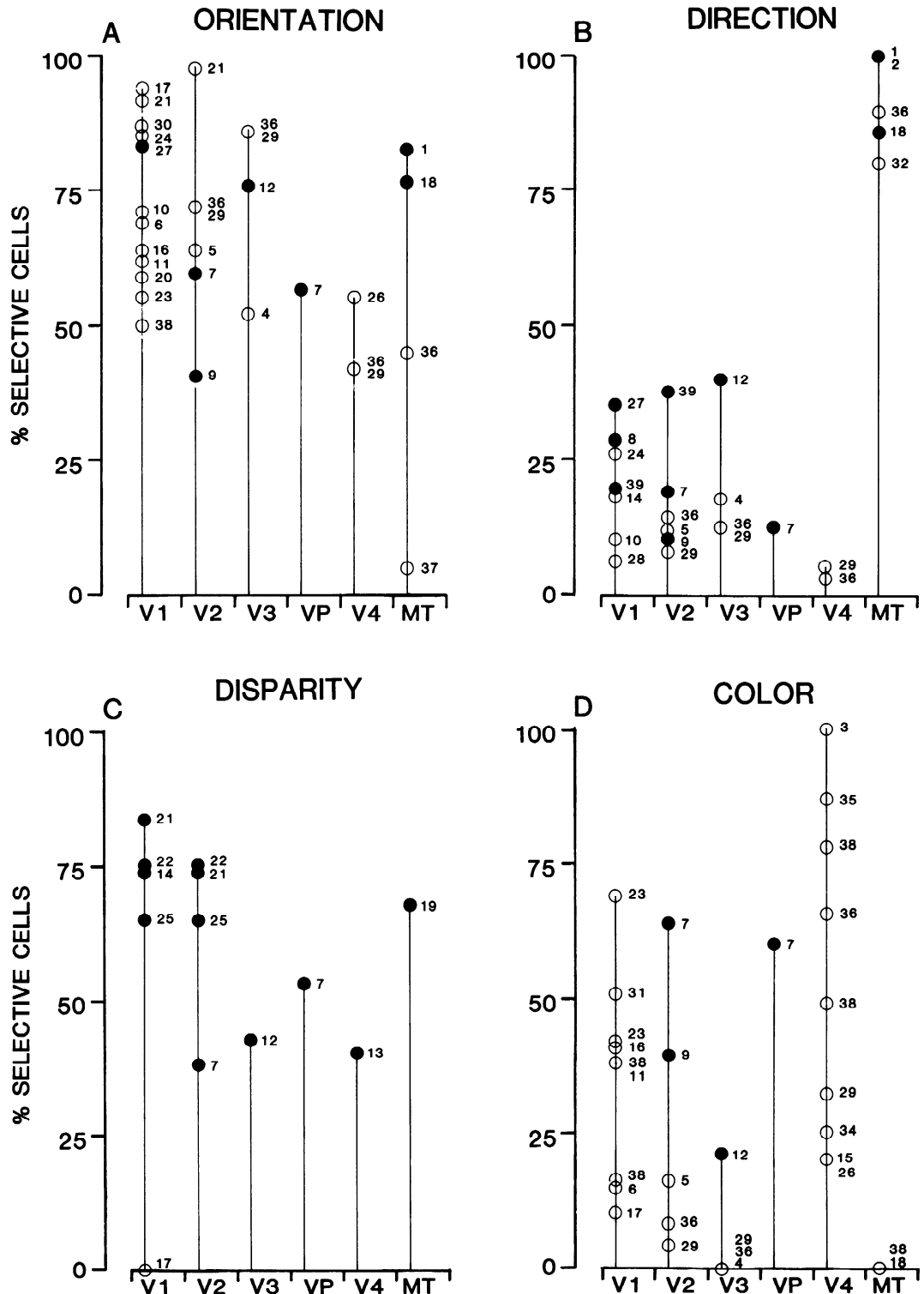


FIG. 16. Functional streams in visual cortex. Anatomical hierarchy of magnocellular (shaded) and parvocellular functional streams from retina to parietal and inferotemporal cortex. V1 is subdivided into three levels corresponding to the interlaminar flow of information. The dotted line from V2 thick stripe compartment to V3 denotes an expected but undemonstrated projection. Inferotemporal cortex is indicated by a single box, but our recent work strongly indicates multiple subdivisions within this brain region.

with results of Zeki (89) and Van Essen and Zeki (81) but is significantly greater than Baizer's (5) estimate of 48%, possibly owing to differences in recording conditions (hers were awake, behaving monkeys). Orientation selectivity is relatively high in all cortical areas studied to date (Fig. 17A). Given that the variability of estimates within an area is comparable to that between areas, it is unclear whether there are any genuine differences on an area by area basis. Within subregions of a

given area, however, there can be large differences, the most notable being the generally nonoriented cells in the cytochrome oxidase-rich blobs of V1 versus the highly orientation-selective cells in the superficial interblob regions (44). The evidence for V2 is more sketchy, but there may also be higher orientation selectivity in interstripes and thick stripes than in thin cytochrome oxidase stripes (18, 39, 70). Finally, there is a hint that orientation selectivity is higher in areas with little



color selectivity. Thus areas VP and V4, which have a high incidence of color selectivity, have less orientation selectivity than area MT, which lacks color selectivity, and area V3, which has a small amount of color selectivity.

DIRECTION. We were initially surprised to find that 40% of V3 cells show strong direction selectivity. Previous qualitative investigations estimated direction selectivity to be much less prevalent in V3 (12–15%, Refs. 5, 81). In the present experiments, if all cells with at least a direction bias are considered ($DI > 0.5$; 2:1 response ratio), then 61% of V3 cells are direction selective. Figure 17B summarizes what is known about direction selectivity in macaque visual cortex and illustrates that, unlike orientation selectivity, high incidences of direction selectivity are not observed throughout visual cortex. Estimates of direction selectivity in V1 are, in general, fragmentary and vary widely across qualitative (i.e., 6%, Ref. 72) and quantitative studies (i.e., 35%, Ref. 66).

The highest incidence of direction selectivity in extrastriate cortex is observed in area MT where qualitative and quantitative estimates range from 84 to 100% (2, 87). In contrast, other extrastriate areas have much lower incidences of direction selectivity (3–19%, V4, Ref. 25; ventral V2, Ref. 10). Direction selectivity in V2 is more frequently encountered

in the thick cytochrome oxidase stripes, which provide input to area MT (18). These results suggest that MT, and probably area V3, owing to their high proportion of direction selectivity, are closely involved in the analysis of motion.

DISPARITY. Selectivity for local binocular disparity has frequently been encountered throughout visual cortex (Fig. 17C). In V1, Hubel and Wiesel (41) reported an absence of disparity selectivity in anesthetized monkeys, but Poggio and collaborators have demonstrated that 60–84% of V1 cells are tuned for disparity in the awake behaving animal (60, 62). Comparably high proportions have been reported for extrastriate areas V2 and MT (10, 49, 60). In the present study, 43% of V3 neurons were disparity selective. This value is similar to Burkhalter and Van Essen's (10) estimate of 53% in area VP and our preliminary estimate of 30–50% in V4 (Felleman and Van Essen, unpublished observations).

In addition to their selectivity for binocular disparity using solid contours, many cortical neurons are also capable of responding to random dot stereograms. In agreement with our study using solid contours, Poggio (56) reported that 30–35% of cells in V1 and, most remarkably, 70–75% of cells probably located in V3, are tuned for disparity in these dynamic stereograms. This suggests that V3 may be

FIG. 17. Comparison of neuronal selectivities across visual cortical areas. Estimates of the proportion of cells in different cortical areas selective for *A*, orientation; *B*, direction; *C*, binocular disparity; and *D*, color. Qualitative estimates indicated by open symbols and quantitative estimates by solid symbols. Numbers beside each symbol refer to individual published studies as indicated below.

1. Albright ('84)
2. Albright et al. ('84)
3. Anderson et al. ('82)
4. Baizer ('82)
5. Baizer et al. ('77)
6. Bullier and Henry ('80)
7. Burkhalter and Van Essen ('86)
8. DeValois et al. ('82)
9. DeYoe and Van Essen ('85)
10. Dow ('74)
11. Dow and Gouras ('73)
12. Felleman and Van Essen (present study)
13. Felleman and Van Essen (unpublished)
14. Fischer and Poggio ('79)
15. Fischer et al. ('81)
16. Gouras ('74)
17. Hubel and Wiesel ('68)
18. Maunsell and Van Essen ('83a)
19. Maunsell and Van Essen ('83b)
20. Poggio ('72)
21. Poggio and Fischer ('77)
22. Poggio and Talbot ('81)
23. Poggio et al. ('75)
24. Poggio et al. ('77)
25. Poggio et al. ('85)
26. Schein et al. ('82)
27. Schiller et al. ('76)
28. Spinelli et al. ('70)
29. Van Essen and Zeki ('78)
30. Wurtz ('69)
31. Yates ('74)
32. Zeki ('74)
33. Zeki ('73)
34. Zeki ('75)
35. Zeki ('77)
36. Zeki ('78)
37. Zeki ('80)
38. Zeki ('83)
39. Foster et al. ('85)

particularly involved in several aspects of stereopsis.

COLOR. The proportion of color-selective cells varies considerably across cortical areas (Fig. 17*D*). In the present study, 21% of V3 cells were found to be color selective using our quantitative criteria. In contrast, previous qualitative investigations in V3 reported no color selectivity (5, 81). Overall estimates of color selectivity in V1 and V2 range from <10% to nearly 70% (in foveal V1). Much of the variability in these estimates is due to differences in criteria as well as apparent heterogeneity in the distributions of color selective cells. In V1, color-selective cells are segregated both by layer and in the horizontal domain relative to cytochrome oxidase blobs (44, 52). In V2, color-selective cells are primarily concentrated in cytochrome oxidase thin stripe and interstripe regions (18). V3 receives feed-forward inputs from V1 and V2, and it seems possible that the color selectivity observed in V3 arises from specific V2 inputs. Given that almost all color-selective cells in V3 are also orientation selective, the interstripe compartment of V2 is a possible source of this input (18). Alternatively, color selectivity might arise from the subpopulation of color-selective cells in layer 4B of V1 reported by Michael (52). A high incidence of color selectivity is found in two other targets of V2, including a majority of cells in both areas VP and V4. Finally, no color selectivity whatsoever has been reported for area MT (e.g., Ref. 48), although it has not been tested extensively in the quantitative ways we have used for V3 and VP.

SPEED. Most neurons in all visual cortical areas are highly responsive to movement, and, when tested, most cells show clear preferences for specific rates of motion. In the present study neurons in V3 were almost all tuned for the speed of movement and almost half preferred a speed of 16°/s. Using the same testing paradigm, other studies from this laboratory have found modal preferred speeds of 8°/s in V1 (Fig. 9, Ref. 76), 32°/s in VP (10), and 32°/s in MT (48). [A modal value of 32°/s was reported for 13 cells in V2 (10), but this estimate may be inaccurate given the very small sample size.] There is an overall tendency for higher-speed preferences to be associated with areas having larger receptive fields, just as there is a correlation between

preferred speed and eccentricity within an area (48). Presumably, this arises because integration over long distances in the visual field is needed to signal accurate information about high speeds. The higher speed preferences in V3 and MT may also be associated with the predominant input from the magnocellular pathway, whose cells tend to respond transiently and hence poorly to slow speeds (cf. Ref. 22).

The range of preferred speeds that we encountered was surprisingly narrow, with over 80% of V3 cells preferring speeds of 8–32°/s. In comparison, the reported range is slightly broader for VP (10) and broader still for MT (48). These differences may, in part, reflect sampling biases, given that our V3 recordings were strongly clustered around the 2–8° range (cf. Fig. 3), and, as already mentioned, preferred speed is correlated with eccentricity. However, comparison with the same restricted eccentricity range in MT indicates that a broader range of preferred speeds are represented within MT (cf. Fig. 8, Ref. 44).

In summary, the present analysis of the functional properties of neurons in the various subdivisions of visual cortex points out two general types of evidence indicative of separate functional streams in extrastriate cortex. One concerns the differential distribution of color selectivity, particularly its absence in MT and its low incidence in V3. The other concerns direction selectivity, which is most frequently encountered in areas MT and V3, thus implicating the magnocellular stream in motion analysis. On the other hand, analysis of stimulus motion is unlikely to be the sole function of the magnocellular stream, since direction selectivity is only seen in 40% of V3 cells and an even smaller percentage of cells in the V2 thick cytochrome oxidase stripes. This suggests an additional role for the magnocellular stream, possibly including low contrast form analysis.

Additional evidence bearing on this issue comes from patterns of myeloarchitecture. Heavy myelination and/or fast conductional velocity is characteristic of every stage along the magnocellular stream from the retina to the parietal lobe (e.g., 8, 21, 74, 79). This heavy myelination may provide for high temporal resolution and high-speed transmission of signals throughout this pathway (47).

Both areas V3 and MT have major projec-

tions into various subdivisions of the parietal lobe, whereas the major projections of V4 (the parvocellular stream) are to several subdivisions of inferotemporal cortex. However, there is considerable anatomical cross-talk, and there may be substantial physiological cross-talk beyond that seen with the current levels of analysis. For example, V3 has strong patchy connections with V4 that are clearly feedforward in nature (Ref. 26 and in preparation). It is not known if these projections are limited to color-selective V3 cells or is distributed more evenly across V3. Nevertheless, this pathway from V3 to V4 could provide a major route for magnocellularly derived form information to reach the temporal lobe (25–27, 68). Similarly, in addition to its major inputs to the temporal lobe, V4 has connections with several subdivisions of parietal cortex (e.g., Refs. 25, 69).

In assessing the significance of functionally segregated streams of information processing in visual cortex, it will become increasingly important to go beyond the use of general terms like motion or form analysis and to focus on the specific problems that need to be solved by different visual areas. Motion processing and form analysis as applied to real-life patterns require many complex computations based on various sources of information (see Ref. 54). Some problems may be solved independently within either the magnocellular or parvocellular streams, but others may require convergent information. Each extrastriate visual area may be performing several different computational tasks, with the nature and the source of information varying from area to area. Thus the notion of functional streams may simply define the source of information and limit the available computations within a given area. However, many different computational tasks can be performed within both the magnocellular and parvocellular streams.

Multipeaked orientation and direction tuning: higher-order form and/or motion analysis?

One of the more striking properties encountered in some V3 neurons was a multipeaked orientation and/or direction tuning. These cells showed narrow tuning for two or more orientations or nonaxial directions when tested with a single flashed or moving bar. Cells

somewhat analogous to these were first described in cat area 19 and were termed "higher-order hypercomplex cells" (40). Their distinguishing characteristic was a selectivity for two orientations differing by 90°. This property led Hubel and Wiesel to suggest that such cells may represent a higher level of form analysis; for example signaling the presence of a corner in the receptive field. These cells, like the multipeaked cells in V3, were rarely encountered (only 11 cells in total) but, when found, they occurred in clusters.

The multipeaked orientation and direction selective cells in V3 differ in one major respect from the higher-order hypercomplex cells of cat area 19. Unlike higher-order hypercomplex cells, the multiple orientation or direction components of these V3 cells were not necessarily at right angles to each other (for example, see Figs. 10A and 11A). However, like some higher-order hypercomplex cells (Ref. 40, cf. Fig. 25), some of these V3 neurons were direction selective. Finally, it remains to be determined whether these cells in V3 share the spatial generalization within their receptive field like that described for higher-order hypercomplex cells.

Multiple peaks in direction-tuning curves were also described by Hammond (38) for some cells in cat area 17. In these experiments, multiple direction peaks were observed for some complex cells (particularly in the infragranular layers) when stimulated with a moving pattern of visual noise (cf. Fig. 1). This observation was dependent on stimulus speed; a broad unimodal response peak typically gave rise to a bimodal form as stimulus speed was increased. The notch between the two peaks would correspond to the preferred direction for bar movement. While these results were interpreted to indicate the independence of orientation- and direction-selective mechanisms, they might also be explained on the basis of simple orientation and speed selectivity. Accordingly, the decrease in response to noise at the preferred direction of bar movement when speed is increased might be due to the resultant high temporal frequencies in the stimulus exceeding the temporal frequency bandpass of the cell.

In monkeys, multipeaked direction-tuning curves were observed by DeValois et al. (17) for a small minority of neurons in V1 when tested with single moving bars. These cells

were characterized by narrow orientation/direction tuning, maximum inhibition <90° away from the peak response, and secondary excitatory lobes ranging in amplitude from minor to nearly equivalent to the peak response. These authors suggested that multi-peaked tuning curves represent one end of a continuum of response types with the other end characterized by simple, single-peak orientation selectivity. In their derived models, the presence of secondary excitatory peaks was attributed to secondary excitatory domains falling outside the conventional inhibitory flanks of simple striate neurons. It seems possible that the multipeak cells we encountered in V3 acquired their properties by convergent inputs from such cells in V1.

Finally, Albright (1) found that a minority of neurons in area MT of macaques have unusual orientation and direction tuning. He described two populations of neurons that differed in their relationships between preferred orientation, determined with static slits, and preferred direction, determined with moving slits. Type I MT neurons had orientation preferences orthogonal to their preferred direction of motion. Type II cells, in contrast, displayed an orientation preference parallel to the preferred direction. For some of these latter cells, reduction of stimulus speed led to a multi-peaked direction-tuning curve. Albright has argued that these type II MT neurons (3) represent a higher level of motion analysis corresponding to a pattern direction selectivity rather than a selectivity for individual oriented contours along the lines previously analyzed by Movshon et al. (53). According to his results and subsequent modeling, the expression of a multi-peaked direction-tuning curve following a reduction of component speed is predicted for a pattern selective neuron with a velocity band-pass response.

A critical issue to address for these multi-peaked cells in V1, V3, and MT, is whether or not they all relate to a similar type of higher-order motion analysis. The multiple peaks in some V3 cells when tested with flashed bars were notably different from those reported for type II MT cells. Furthermore, when tested, orientation and direction peaks were at least in some cases orthogonal, rather than parallel as is seen in type II MT cells. This suggests that multi-peaked V3 cells do not provide a dominant input to the type II MT neurons.

Thus, whatever role, if any, the multipeak direction cells of V3 have in complex motion analysis, it may be of a qualitatively different type than that discussed for MT by Movshon et al. (53) and Albright (1, 3).

Distinctions between areas V3 and VP

Area V3 was first described as a narrow strip of cortex immediately anterior to both dorsal and ventral V2 and thus representing the lower and upper visual fields, respectively (12, 84). Over the last several years, this laboratory has obtained a variety of anatomical and physiological lines of evidence that indicate two separate subdivisions within this strip; V3 dorsally and VP, the ventral posterior area, ventrally. These observations have been presented in detail elsewhere (9) and will be summarized and augmented here.

Anatomical evidence for a dorsoventral asymmetry within the strip anterior to V2 has come from studies of connections with V1. Specifically, dorsal V1 is reciprocally connected with V3 but ventral V1 has no corresponding connection with VP (9, 11, 26, 80). A second important anatomical asymmetry comes from the analysis of cortical myeloarchitecture. In short, V3 is densely myelinated, whereas VP is not (9, 80).

Major population differences in receptive field properties emerge from a comparison of the present results on V3 with those previously acquired by Burkhalter and Van Essen (10) for VP. Cells in both areas were tested using essentially identical bias-free methods to determine their selectivities to stimulus color, orientation, direction, speed, and binocular disparity.

Although a variety of differences exist between these two populations, the most striking differences relate to selectivity for direction of stimulus motion and for stimulus color. Using a criterion value of 0.7 on the direction index to indicate strong direction selectivity, 40% of the neurons in V3 but only 13% of VP neurons were strongly direction selective. This difference in proportions is highly statistically significant ($P < 0.0005$), as is the difference in the mean direction index for the V3 and VP populations. Concerning color selectivity, 21% of the neurons in V3 and 64% of neurons in VP are color selective, using a criterion of 0.7 for the color index. Again, this difference is highly statistically significant ($P < 0.0005$), as

is the difference in the mean color index for the two populations. These differences are not attributable to sampling closer to the fovea in the VP sample compared with the V3 sample. In fact, the sampling bias is in the opposite direction, with the V3 population sampled more centrally than VP. This counterbias might serve to reduce the observed difference between V3 and VP if color selectivity were inversely related to eccentricity. However, the available data indicate that lower color indexes are not associated with greater eccentricities in area VP (10).

Our reliance on a color index based on maximum vs. minimum responses at different wavelengths has the disadvantage of not providing a rigorous measure of the statistical significance of the index value for any given cell. Given the small number of stimulus repetitions (3–5) at each wavelength, random fluctuations in responsiveness would tend to produce irregular, nonflat response curves. Thus it seemed conceivable that the color indexes in VP were higher than in V3 because the data were noisier, rather than because the cells were genuinely more color selective. Although this possibility seemed remote, we ruled it out explicitly by using an analysis of variance to determine the probability that each color response curve was significantly deviant from flatness. For each cell tested quantitatively for color selectivity in areas V3 and VP the variance in response across wavelengths was compared with the average variance across different trials at the same wavelength. The resultant *F* statistic (30) is significant when the variance in responses between different wavelengths is approximately twice the average variance of responses for repetitions of the same wavelength (for 3–5 repetitions of 11 different wavelengths, $P < 0.05$; critical values of *F* range from 1.92 to 2.18). The vast majority of V3 cells had *F* values below the criterion level. A few cells (5/106; 4.8%) had statistically significant *F* values ($P < 0.05$), but this propor-

tion would be expected by chance alone. In contrast, nearly half of the VP population had statistically significant *F* values (36/77; 47%).

As an assay for color selectivity per se, the analysis of variance used here is overly stringent, because it does not take into consideration trends or clustering of high or low responses as a function of wavelength. Thus it somewhat underestimates the proportion of cells showing genuine color selectivity. Nevertheless, this analysis provides a useful confirmation that V3 and VP differ importantly in their processing of color information.

In summary, we find a variety of anatomical and physiological asymmetries in the cortical strip anterior to dorsal and ventral V2. These differences are large enough to warrant separate nomenclature for the dorsal and ventral subdivisions. We have chosen to label the dorsal zone V3, based on its historical association as a V1 projection zone anterior to V2. VP, in ventral extrastriate cortex, is thus distinguished from the dorsally located V3 by a variety of criteria. This terminology implies that these two separate visual areas each only represents half of the visual field; the lower field in V3 and upper field in VP. This functional asymmetry suggests that psychophysical asymmetries should exist between the upper and lower visual fields. Indeed, modest upper vs. lower field perceptual asymmetries have been reported in humans (71; see also Ref. 9).

ACKNOWLEDGMENTS

We are grateful to Dr. A. Burkhalter, Dr. E. DeYoe, and G. Carman for assistance during some of the recording sessions. We also thank C. Shotwell and K. Tazumi for histological work and preparation of figures. In addition, we thank C. Hochenedel, C. Oto, and L. Finger for preparation of the manuscript. Finally, we thank Dr. J. H. R. Maunsell and an anonymous reviewer for helpful comments on the manuscript.

This work was supported by National Eye Institute Research Grant R01 EY-02091 to D. Van Essen.

Received 20 March 1986; accepted in final form 23 October 1986.

REFERENCES

- ALBRIGHT, T. D. Direction and orientation selectivity of neurons in visual area MT of the macaque. *J. Neurophysiol.* 52: 1106–1130, 1984.
- ALBRIGHT, T. D., DESIMONE, R., AND GROSS, C. Columnar organization of directionally selective cells in visual area MT of the macaque. *J. Neurophysiol.* 51: 16–31, 1984.
- ALBRIGHT, T. D., RODMAN, H. R., AND GROSS, C. G. Type II MT neurons show pattern-motion direction selectivity. *Soc. Neurosci. Abstr.* 12: 1369, 1986.
- ANDERSON, V. V., GULD, C., AND SJÖ, O. Colour processing in prestriate cortex of vervet monkey. In: *Colour Vision*, edited by J. D. Mollon and L. T. Sharpe. London: Academic, 1983.
- BAIZER, J. S. Receptive field properties of V3 neurons

- in monkey. *Invest. Ophthalmol. Visual Sci.* 23: 87-95, 1982.
6. BAIZER, J. S., ROBINSON, D. L., AND DOW, B. M. Visual responses of area 18 neurons in awake, behaving monkey. *J. Neurophysiol.* 40: 1024-1037, 1977.
 7. BALLARD, D. H. Cortical connections and parallel processing: Structure and function. *Behav. Brain Sci.* 9: 67-120, 1986.
 8. BULLIER, J. AND HENRY, G. H. Ordinal position and afferent input of neurons in monkey striate cortex. *J. Comp. Neurol.* 193: 913-935, 1980.
 9. BURKHALTER, A., FELLEMAN, D. J., NEWSOME, W. T., AND VAN ESSEN, D. C. Anatomical and physiological asymmetries related to visual areas V3 and VP in macaque extrastriate cortex. *Vision Res.* 26: 63-80, 1986.
 10. BURKHALTER, A. AND VAN ESSEN, D. C. Processing of color, form and disparity in visual areas V2 and VP of ventral extrastriate cortex in the macaque. *J. Neurosci.* 6: 2327-2351, 1986.
 11. BURKHALTER, A. AND VAN ESSEN, D. C. The connections of the ventral posterior area (VP) in the macaque monkey. *Soc. Neurosci. Abstr.* 9: 153, 1983.
 12. CRAGG, B. G. The topography of the afferent projections in the circumstriate visual cortex of the monkey studied by the Nauta method. *Vision Res.* 9: 733-747, 1969.
 13. CYNADER, M. AND REGAN, D. Neurons in cat parastriate cortex sensitive to the direction of motion in three-dimensional space. *J. Physiol. Lond.* 274: 549-569, 1978.
 14. DERRINGTON, A. M., KRAUSKOPF, J., AND LENNIE, P. Chromatic mechanisms in lateral geniculate nucleus of macaque. *J. Physiol. Lond.* 357: 241-265, 1984.
 15. DERRINGTON, A. M. AND LENNIE, P. Spatial and temporal contrast sensitivities of neurons in lateral geniculate nucleus of macaque. *J. Physiol. Lond.* 357: 219-240, 1984.
 16. DESIMONE, R., FLEMING, J., AND GROSS, C. G. Parastriate afferents to inferior temporal cortex: an HRP study. *Brain Res.* 184: 41-55, 1980.
 17. DEVALOIS, R., YUND, E. W., AND HELPER, N. The orientation and direction selectivity of cells in macaque visual cortex. *Vision Res.* 22: 531-544, 1982.
 18. DEYOE, E. A. AND VAN ESSEN, D. C. Segregation of efferent connections and receptive field properties in visual area V2 of the macaque. *Nature Lond.* 317: 58-61, 1985.
 19. DOW, B. M. Functional classes of cells and their laminar distribution of monkey visual cortex. *J. Neurophysiol.* 37: 927-946, 1974.
 20. DOW, B. M. AND GOURAS, P. Color and spatial specificity of single units in rhesus monkey foveal striate cortex. *J. Neurophysiol.* 36: 79-100, 1974.
 21. DREHER, B., FUKUDA, Y., AND RODIECK, R. W. Identification, classification and anatomical segregation of cells with X-like and Y-like properties in the lateral geniculate nucleus of old-world primates. *J. Physiol. Lond.* 25: 433-452, 1976.
 22. DUYSENS, J., ORBAN, G. A., CREMIEUX, J., AND MAES, H. Velocity selectivity in the cat visual system. III. Contribution of temporal factors. *J. Neurophysiol.* 54: 1068-1083, 1985.
 23. FELLEMAN, D. J., CARMAN, G. J., AND VAN ESSEN, D. C. Evidence for a functional distinction between areas V3 and VP of macaque extrastriate cortex. *Invest. Ophthalmol. Visual Sci. Suppl.* 25: 278, 1984.
 24. FELLEMAN, D. J., DEYOE, E. A., AND VAN ESSEN, D. C. Two topographically organized visual areas in ventral extrastriate cortex of the macaque. *Soc. Neurosci. Abstr.* 11: 1246, 1985.
 25. FELLEMAN, D. J. AND VAN ESSEN, D. C. The connections of area V4 of macaque extrastriate cortex. *Soc. Neurosci. Abstr.* 9: 153, 1983.
 26. FELLEMAN, D. J. AND VAN ESSEN, D. C. Cortical connections of area V3 in macaque extrastriate cortex. *Soc. Neurosci. Abstr.* 10: 933, 1984.
 27. FENSTEMAKER, S. B., OLSON, C. R., AND GROSS, C. G. Afferent connections of macaque visual areas V4 and TEO. *Invest. Ophthalmol. Visual Sci. Suppl.* 25: 213, 1984.
 28. FISCHER, B., BOCH, R., AND BACH, M. Stimulus versus eye movements: comparison of neural activity in the striate and prelunate visual cortex (A17 and A19) of trained rhesus monkey. *Exp. Brain Res.* 43: 69-78, 1981.
 29. FISCHER, B. AND POGGIO, G. F. Depth sensitivity of binocular cortical neurons of behaving monkeys. *Proc. R. Soc. Lond. B Biol. Sci.* 204: 409-414, 1979.
 30. FISHER, A. M. *Statistical Methods for Research Workers*. Edinburgh: Oliver & Boyd, 1954.
 31. FOSTER, K. H., GASKA, J. P., NAGLER, M., AND POLLEN, D. A. Spatial and temporal frequency selectivity of neurons in VI and VII of the macaque monkey. *J. Physiol. Lond.* 365: 331-363, 1985.
 32. GALLYAS, F. Silver staining of myelin by means of physical development. *Neurol Res.* 1: 203-209, 1979.
 33. GATTASS, R., GROSS, C. G., AND SANDELL, J. H. Visual topography of V2 in the macaque. *J. Comp. Neurol.* 201: 519-539, 1981.
 34. GATTASS, R., SOUSA, A. P. B., AND COVEY, E. Cortical Visual Areas of the macaque: possible substrates for pattern recognition mechanisms. In: *Study Group on Pattern Recognition Mechanisms*, edited by C. Chagas. Vatican City: Pontifical Acad. Sci., 1985, p. 1-20.
 35. GILBERT, C. D. Laminar differences in receptive field properties of cells in cat primary visual cortex. *J. Physiol. Lond.* 268: 391-421, 1977.
 36. GIZZI, M. S., NEWSOME, W. T., AND MOVSHON, J. A. Directional selectivity of neurons in macaque MT. *Invest. Ophthalmol. Visual Sci. Suppl.* 24: 104, 1983.
 37. GOURAS, P. Opponent-colour cells in different layers of foveal striate cortex. *J. Physiol. Lond.* 238: 583-602, 1974.
 38. HAMMOND, P. Directional tuning of complex cells in area 17 of the feline visual cortex. *J. Physiol. Lond.* 285: 479-491, 1978.
 39. HUBEL, D. H. AND LIVINGSTONE, M. S. Complex-unoriented cells in a subregion of primate area 18. *Nature Lond.* 315: 325-327, 1985.
 40. HUBEL, D. H. AND WIESEL, T. N. Receptive fields and functional architecture in two nonstriate visual areas (18 and 19) of the cat. *J. Neurophysiol.* 28: 229-289, 1965.
 41. HUBEL, D. H. AND WIESEL, T. N. Receptive fields and functional architecture of monkey striate cortex. *J. Physiol. Lond.* 195: 215-243, 1968.

42. HUBEL, D. H. AND WIESEL, T. N. Cells sensitive to binocular depth in area 18 of the macaque monkey cortex. *Nature Lond.* 225: 41-42, 1970.
43. KAPLAN, E. AND SHAPLEY, R. M. X and Y cells in the lateral geniculate nucleus of macaque monkeys. *J. Physiol. Lond.* 330: 125-143, 1982.
44. LIVINGSTONE, M. S. AND HUBEL, D. H. Anatomy and physiology of a color system in the primate visual cortex. *J. Neurosci.* 4: 309-356, 1984.
45. LUND, J. S. Intrinsic organization of the primate visual cortex, area 17, as seen in Golgi preparations. In: *The Organization of the Cerebral Cortex*, edited by F. O. Schmitt, F. G. Worden, G. Adelman, and S. G. Dennis. Cambridge, MA: MIT Press, 1981, p. 105-124.
46. MALPELI, J. G., SCHILLER, P. H., AND COLBY, C. L. Response properties of single cells in monkey striate cortex during reversible inactivation of individual lateral geniculate laminae. *J. Neurophysiol.* 46: 1102, 1981.
47. MAUNSELL, J. H. R. Physiological evidence for two visual subsystems. In: *Matters of Intelligence*, edited by L. Vaina. Dordrecht, Netherlands: Reidel Press.
48. MAUNSELL, J. H. R. AND VAN ESSEN, D. C. Functional properties of neurons in middle temporal visual area of the macaque monkey. I. Selectivity for stimulus direction, speed, and orientation. *J. Neurophysiol.* 49: 1127-1147, 1983a.
49. MAUNSELL, J. H. R. AND VAN ESSEN, D. C. Functional properties of neurons in middle temporal visual area of the macaque monkey. II. Binocular interactions and sensitivity to binocular disparity. *J. Neurophysiol.* 49: 1148-1167, 1983b.
50. MAUNSELL, J. H. R. AND VAN ESSEN, D. C. The connections of the middle temporal visual area (MT) and their relationship to a cortical hierarchy in the macaque monkey. *J. Neurosci.* 3: 2563-2686, 1983c.
51. MICHAEL, C. R. Columnar organization of color cells in monkey's striate cortex. *J. Neurophysiol.* 46: 587, 1981.
52. MICHAEL, C. R. Laminar segregation of color cells in the monkey's striate cortex. *Vision Res.* 25: 415-423, 1985.
53. MOVSHON, J. A., ADELSON, E. H., GIZZI, M. S., AND NEWSOME, W. T. The analysis of moving visual patterns. In: *Study Group on Pattern Recognition Mechanisms*, edited by C. Chagas. Vatican City: Pontifical Acad. Sci., 1985, p. 117-151.
54. NAKAYAMA, K. Biological image motion processing: a review. *Vision Res.* 25: 625-660, 1985.
55. NEWSOME, W. T., MAUNSELL, J. H. R., AND VAN ESSEN, D. C. The ventral posterior visual area of the macaque: Visual topography and areal boundaries. *J. Comp. Neurol.* 252: 139-153, 1986.
56. POGGIO, G. F. Cortical mechanisms of stereopsis. *Invest. Ophthalmol. Visual Sci.* 26: 133, 1985.
57. POGGIO, G. F. Spatial properties of neurons in striate cortex of unanesthetized macaque monkey. *Invest. Ophthalmol.* 11: 368-377, 1972.
58. POGGIO, G. F., BAKER, F. H., MANSFIELD, R. J. W., SILLITO, A., AND GRIGG, P. Spatial and chromatic properties of neurons subserving foveal and parafoveal vision in rhesus monkey. *Brain. Res.* 100: 25-59, 1975.
59. POGGIO, G. F., DOTY, R. W., JR., AND TALBOT, W. H. Foveal striate cortex of behaving monkey: single-neuron responses to square-wave gratings during fixation of gaze. *J. Neurophysiol.* 40: 1369, 1977.
60. POGGIO, G. F. AND FISCHER, B. Binocular interaction and depth sensitivity in striate and prestriate cortex of behaving rhesus monkey. *J. Neurophysiol.* 40: 1392-1405, 1977.
61. POGGIO, G. F., MOTTER, B. C., SQUATRITO, S., AND TROTTER, Y. Responses of neurons in visual cortex (V1 and V2) of the alert macaque to dynamic random-dot stereograms. *Vision Res.* 25: 397-406, 1985.
62. POGGIO, G. F. AND TALBOT, W. H. Mechanisms of static and dynamic stereopsis in foveal cortex of the rhesus monkey. *J. Physiol. Lond.* 315: 469-492, 1981.
63. ROCKLAND, K. S. AND PANDYA, D. N. Laminar origins and terminations of cortical connections of the occipital lobe in the rhesus monkey. *Brain Res.* 179: 3-20, 1979.
64. ROSE, D. Responses of single units in cat visual cortex to bar of light as a function of bar length. *J. Physiol. Lond.* 271: 1-23, 1977.
65. SCHEIN, S. J., MARROCCO, R. T., AND DE MONASTERIO, F. M. Is there a high concentration of color-selective cells in area V4 of monkey visual cortex? *J. Neurophysiol.* 47: 193, 1982.
66. SCHILLER, P. H., FINLAY, B. L., AND VOLMAN, S. F. Quantitative studies of single-cell properties in monkey striate cortex. I. Spatiotemporal organization of receptive fields. *J. Neurophysiol.* 39: 1288-1319, 1976a.
67. SCHILLER, P. H., FINLAY, B. L., AND VOLMAN, S. F. Quantitative studies of single-cell properties in monkey striate cortex. II. Orientation specificity and ocular dominance. *J. Neurophysiol.* 39: 1320-1333, 1976b.
68. SELTZER, B. AND PANDYA, D. N. Some cortical projections to the parahippocampal area in the rhesus monkey. *Exp. Neurol.* 50: 146-160, 1976.
69. SELTZER, B. AND PANDYA, D. N. Converging visual and somatic sensory cortical input to the intraparietal sulcus of the rhesus monkey. *Brain Res.* 192: 339-351, 1980.
70. SHIPP, S. D. AND ZEKI, S. Segregation of pathways leading from area V2 to areas V4 and V5 of macaque monkey visual cortex. *Nature Lond.* 315: 322-324, 1985.
71. SKRANDIES, W. Human contrast sensitivity: Regional differences. *Human Neurobiol.* 4: 97-99, 1985.
72. SPINELLI, D. N., PRIBRAM, K. H., AND BRIDGEMAN, B. Visual receptive field organization of single units in the visual cortex of monkey. *Int. J. Neurosci.* 1: 67-74, 1970.
73. TOOTELL, R. H., HAMILTON, S. L., SWITKES, E., AND DEVALOIS, R. L. 2DG as a "functional HRP" in macaque striate cortex. *Invest. Ophthalmol. Visual Sci. Suppl.* 26: 8, 1985.
74. UNGERLEIDER, L. G. AND DESIMONE, R. Cortical connections of visual area MT in the macaque. *J. Comp. Neurol.* 248: 190-222, 1986.
75. UNGERLEIDER, L. G. AND MISHKIN, M. Two cortical visual systems. In: *Analysis of Visual Behavior*, edited by D. J. Ingle, M. A. Goodale, and R. J. W. Mansfield. Cambridge, MA: MIT Press, 1982, p. 549-586.
76. VAN ESSEN, D. C. Functional organization of primate visual cortex. In: *Cerebral Cortex*, edited by E. G. Jones and A. A. Peters. New York: Plenum, 1985, vol. 3, p. 259-329.
77. VAN ESSEN, D. C. AND MAUNSELL, J. H. R. Two-

- dimensional maps of the cerebral cortex. *J. Comp. Neurol.* 191: 255-281, 1980.
78. VAN ESSEN, D. C. AND MAUNSELL, J. H. R. Hierarchical organization and functional streams in the visual cortex. *Trends Neurosci.* 6: 370-375, 1983.
79. VAN ESSEN, D. C., MAUNSELL, J. H. R., AND BIXBY, J. L. The middle temporal visual area in the macaque: myeloarchitecture, connections, functional properties and topographic organization. *J. Comp. Neurol.* 199: 293-326, 1981.
80. VAN ESSEN, D. C., NEWSOME, W. T., MAUNSELL, J. H. R., AND BIXBY, J. L. The projections from striate cortex (V1) to visual areas V2 and V3 in the macaque monkey: asymmetries, areal boundaries, and patchy connections. *J. Comp. Neurol.* 244: 451-480, 1986.
81. VAN ESSEN, D. C. AND ZEKI, S. M. The topographic organization of rhesus monkey prestriate cortex. *J. Physiol. Lond.* 277: 193-226, 1978.
82. WIESEL, T. N. AND HUBEL, D. H. Spatial and chromatic interactions in the lateral geniculate body of the rhesus monkey. *J. Neurophysiol.* 29: 1115-1156, 1966.
83. YATES, J. T. Chromatic information processing in the foveal projection (area striata) of unanesthetized primate. *Vision Res.* 14: 163-173, 1974.
84. ZEKI, S. M. Representation of central visual fields in prestriate cortex of monkey. *Brain Res.* 14: 271-291, 1969.
85. ZEKI, S. M. Cortical projections from two prestriate areas in the monkey. *Brain Res.* 34: 19-35, 1971.
86. ZEKI, S. M. Colour coding in rhesus monkey prestriate cortex. *Brain Res.* 53: 422-427, 1973.
87. ZEKI, S. M. Functional organization of a visual area in the posterior bank of the superior temporal sulcus of the rhesus monkey. *J. Physiol. Lond.* 236: 549-573, 1974.
88. ZEKI, S. M. Colour coding in the superior temporal sulcus of rhesus monkey visual cortex. *Proc. R. Soc. Lond. B Biol. Sci.* 197(B): 195-223, 1977.
89. ZEKI, S. M. Uniformity and diversity of structure and function in rhesus monkey prestriate visual cortex. *J. Physiol. Lond.* 277: 273-290, 1978.
90. ZEKI, S. The distribution of wavelength and orientation selective cells in different areas of monkey visual cortex. *Proc. R. Soc. Lond. B Biol. Sci.* 217: 449-470, 1983.